

“I hereby declare that I have read through this report entitle “Simulation of Direct Torque Control of induction machine using 3-level Cascaded H-Bridge Multilevel Inverter” and found that it has comply the partial fulfilment for awarding the degree of Bachelor of Electrical Engineering (Power Electronic and Drives)”.

Signature	:
Supervisor's Name	:	Dr.AUZANI BIN JIDIN
Date	:	18 JUNE 2014

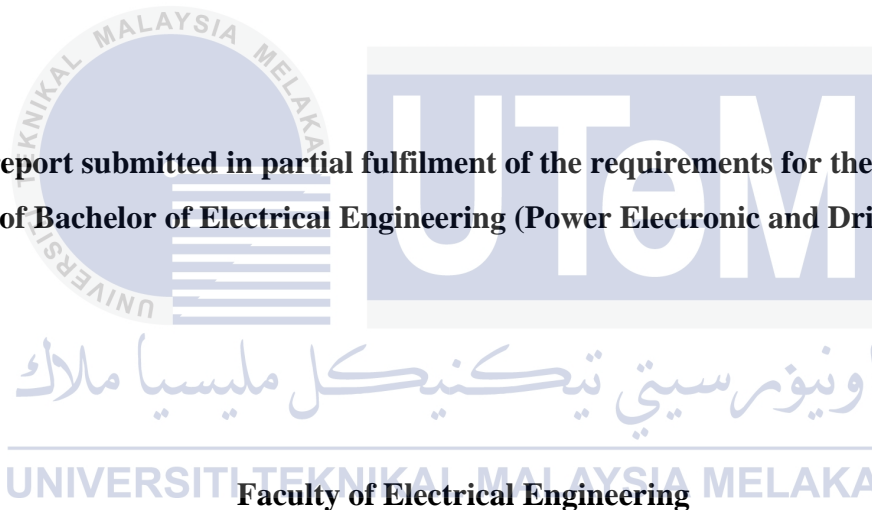
اونيورسيتي تيكنيكل مليسيا ملاك

UNIVERSITI TEKNIKAL MALAYSIA MELAKA

**SIMULATION OF DIRECT TORQUE CONTROL OF INDUCTION MACHINE
USING THREE-LEVEL CASCADED H-BRIDGE MULTILEVEL INVERTER**

MOHAMAD RASYIDI BIN NAZIR ALI

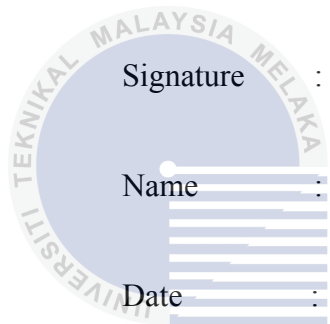
**A report submitted in partial fulfilment of the requirements for the degree
of Bachelor of Electrical Engineering (Power Electronic and Drives)**



UNIVERSITI TEKNIKAL MALAYSIA MELAKA

YEAR 2014

I declare that this report entitle “SIMULATION OF DIRECT TORQUE CONTROL OF INDUCTION MACHINE USING THREE-LEVEL CASCADED H-BRIDGE MULTILEVEL INVERTER” is the result of my own research except as cited in the references. The report has not been accepted for any degree and is not concurrently submitted in candidature of any other degree.

 Signature : _____
Name : MOHAMAD RASYIDI BIN NAZIR ALI
Date : 18 JUNE 2014

اونيورسيتي تيكنيكل مليسيا ملاك

UNIVERSITI TEKNIKAL MALAYSIA MELAKA

ACKNOWLEDGEMENT

Alhamdulillah, I would like to take this opportunity to express my profound gratitude and deep regards to my supervisor, Dr. Auzani Bin Jidin for his exemplary guidance, monitoring and constant encouragement throughout the course of this thesis. The help and guidance given by him time to time shall carry me a long way in the journey of life on which I am about to embark.

I also would like to thanks to all the lecturers that give advice to me especially to both my panel for this Final Year Project. Besides that, I wish to thanks my study partner, Muhd Zharif Rifqi Zuber Ahmadi which gives a lot of idea during this project. I also would like thanks to my fellow course mate for giving me support and share their idea throughout the project.

Last but not least, i would like to express my thanks to my beloved parents, brother and sister for their constant encouragement since beginning my journey in university.

UNIVERSITI TEKNIKAL MALAYSIA MELAKA

ABSTRACT

Direct torque control (DTC) is a method based on vector control that attracts many researchers since it been introduced in 1986. Mostly this method has significant implementation on the induction machine compared to other machine. This is because the simple structure and less parameter required in order performing this mechanism. However, this method has several disadvantages when applying with the two-level inverter such as less selection of effective voltage vector and high switching frequency. This is because the possible number of voltage vector that can be selected is only six. Thus, this problem leads to the losses during the operation of induction machine and increase the torque ripple. Therefore, this research project is to replace the conventional two-level inverter with the cascaded H-Bridge multilevel inverter (CHMI). One of the aims of this project is to formulate an optimal voltage vector selection according to the speed operation for direct torque control of induction machines. Besides that, this project aims to verify the proposed selection of voltage vectors which improve efficiency and reduce torque ripple. In order to achieve the objective, a comprehensive study done by emphasizing on current technical papers to develop the simulation model. First and the foremost, is to construct the induction machine model based on it mathematical equation. By having crystal clear of understanding of the CHMI topology, the next step is to formulate the look-up table. This look-up table consist of three important parameters that are flux magnitudes which control by two-level hysteresis comparator, torque magnitude which control by seven-level hysteresis comparator and the sectors definition of the stator flux plane. In addition, verification of efficiency is done by construct the switching calculation algorithm. The finding highlighted significant improvement of efficiency especially during low speed that is reduction of 61.4% compared to the conventional inverter. The zoom images manage to prove that the torque have reduce significantly compared to conventional.

ABSTRAK

Kawalan tork langsung adalah satu kaedah berdasarkan kawalan vektor yang menarik minat ramai penyelidik sejak ia diperkenalkan pada tahun 1986. Kebanyakan kaedah ini mempunyai pelaksanaan yang ketara pada mesin induksi berbanding dengan mesin lain. Ini adalah kerana strukturnya yang mudah dan parameter yang kurang diperlukan bagi melaksanakan mekanisme ini. Walaubagaimanapun, kaedah ini mempunyai beberapa kelemahan apabila diaplikasikan dengan penyongsang dua tingkat seperti pemilihan vektor voltan yang kurang berkesan dan kekerapan yang tinggi. Ini adalah kerana jumlah kemungkinan vektor voltan yang boleh dipilih hanya enam. Oleh itu, masalah ini membawa kepada kerugian dalam operasi mesin induksi dan meningkatkan gangguan kepada tork. Oleh itu, projek penyelidikan ini adalah untuk menggantikan penyongsang dua peringkat konvensional dengan penyongsang bertingkat H-Bridge. Salah satu matlamat projek ini adalah untuk merumuskan pilihan vektor yang optimum mengikut kelajuan operasi. Selain itu, projek ini bertujuan untuk mengesahkan pemilihan vektor voltan yang betul bagi meningkatkan kecekapan dan mengurangkan gangguan tork. Untuk mencapai objektif ini, satu kajian komprehensif dilakukan dengan memberi penekanan terhadap kertas kerja teknikal semasa untuk membangunkan model simulasi. Langkah pertama adalah untuk membina model mesin induksi berdasarkan persamaan matematik. Dengan mempunyai pemahaman yang terhadap topologi CHMI, langkah seterusnya adalah untuk merangka jadual carian. Jadual carian ini terdiri daripada tiga parameter penting iaitu magnitud fluks yang dikawal oleh dua tahap histerisis comparator, magnitud tork yang dikawal oleh tujuh peringkat histerisis comparator dan definisi sektor. Di samping itu, pengesahan kecekapan dilakukan dengan membina algoritma pengiraan pensuisan. Dapatan menekankan peningkatan yang ketara kecekapan terutamanya semasa kelajuan rendah yang menunjukkan pengurangan sebanyak 61.4% apabila dibandingkan dengan penyongsang konvensional. Imej-imej zoom juga membuktikan gangguan tork juga berjaya dikurangkan.

TABLE OF CONTENTS

CHAPTER	TITLE	PAGE
	ACKNOWLEDGEMENT	i
	ABSTRACT	ii
	ABSTRAK	iii
	TABLE OF CONTENTS	iv
	LIST OF TABLES	vii
	LIST OF FIGURES	viii
	LIST OF APPENDICES	xi
	LIST OF ABBREVIATION	xii
1	INTRODUCTION	1
	1.1 Overview	1
	1.2 Project Motivation	2
	1.3 Objective	3
	1.4 Scope of research	3
	1.5 Report outline	3
2	LITERATURE REVIEW	5
	2.1 Theory	5
	2.1.1 Introduction	5
	2.1.2 Control technique	6
	2.1.3 Conventional three phase voltage sources	
	Inverter (VSI)	7
	2.1.4 Basic principle in direct torque control (DTC)	8
	2.1.5 Types of multilevel inverters	11
	2.5.1.1 Neutral Point Clamped (NPC)	12

TABLE OF CONTENTS

CHAPTER	TITLE	PAGE
	2.5.1.2 Flying capacitor types Multilevel inverters (FCMI)	13
	2.5.1.3 Cascaded H-bridge multilevel Inverter (CHMI)	14
	2.1.6 Inverter performance analysis	15
	2.2 Related previous work	15
	2.3 Summary of review	16
3	METHODOLOGY	17
	3.1 Research Methodology	17
	3.1.1 Introduction	17
	3.1.2 Mathematical model of induction machine	17
	3.1.3 Three phase 3-level Cascaded H-Bridge Multilevel Inverter topology	18
	3.2 Analytical Approach	21
	3.2.1 Design of look-up table for 3-level CHMI	21
	3.2.2 Stator flux and torque estimator	29
	3.2.3 Performing switching frequency calculation Algorithm	30
	3.2.4 Simulation block model of DTC of induction Machine utilizing CHMI	31
	3.2.5 Verification of the effectiveness of the Simulation	32
	3.3 Summary of methodology by flowchart	33

TABLE OF CONTENTS

CHAPTER	TITLE	PAGE
4	RESULT	34
	4.1 Introduction	34
	4.2 Simulation constructed using Matlab	34
	4.3 Simulation results	36
	4.4 Data tabulation of switching frequency	38
	4.5 Three dimensional graph representation	43
	4.6 Waveform result	47
5	CONCLUSION	50
	5.1 Conclusion	50
	5.2 Recommendation	51
	REFERENCES	52
	APPENDICES	55

LIST OF TABLES

TABLE	TITLE	PAGE
2.1	Voltage vector selection table	10
3.1	Number of possible voltage space vector to be selected	20
3.2	Voltage vectors selection table for 3-level CHM Inverter	28
4.1	Motor and control parameter	36
4.2	Switching frequency (Hz) at 300 rpm	40
4.3	Switching frequency (Hz) at 300 rpm	40
4.4	Switching frequency (Hz) at 650 rpm	41
4.5	Switching frequency (Hz) at 650 rpm	41
4.6	Switching frequency (Hz) at 1000 rpm	42
4.7	Switching frequency (Hz) at 1000 rpm	42

LIST OF FIGURES

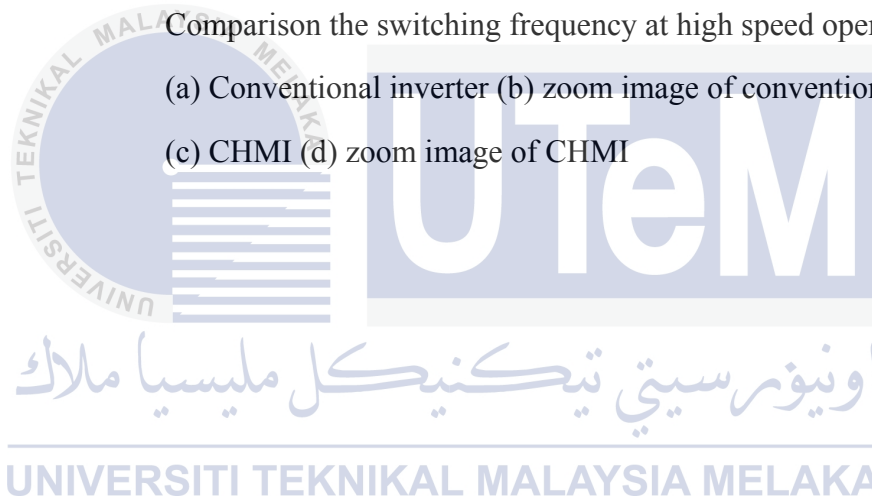
FIGURE	TITLE	PAGE
1.1	Limited voltage vector in conventional inverter lead to Inappropriate selection of switching occurs	2
2.1	Summarization on the evolution of control technique scheme	6
2.2	Topology of Voltage Sources Inverter (VSI)	7
2.3	Voltage space vectors of a 3-phase inverter with the corresponded switching states	8
2.4	Control of flux magnitude using a 2-level hysteresis comparator	8
2.5	Summary of flux error status in hysteresis band	9
2.6	Control of torque using a 3-level hysteresis comparator	9
2.7	Summary of torque error status in hysteresis band	9
2.8	Definition of six sectors of the stator flux plane	10
2.9	A conventional control structure of DTC-hysteresis based induction machine	11
2.10	Three phase three level of neutral point clamped	13
2.11	Three phase three level flying capacitor multilevel inverter	14
2.12	Three levels CHMI connected to 3-phase induction machine	15
3.1	Simplified topology 3 Level Cascaded H-bridge Multilevel Inverter connected to 3-phase induction machine	19
3.2	Typical waveform of the flux, the flux error and the flux error status for the two-level hysteresis torque comparator	22
3.3	Control of torque using a 7-level hysteresis comparator	23
3.4	Summary of torque error status in hysteresis band	23
3.5	Typical waveform of the torque, the torque error and the torque error status for the three-level hysteresis torque comparator	24
3.6	The sector definition of (a) the stator flux plane for long and short voltage vector (b) the stator flux plane for medium	

LIST OF FIGURES

FIGURE	TITLE	PAGE
	voltage vector	25
3.7	Two possible active voltage are switched for each sector to control the stator flux within its hysteresis band	25
3.8	Definition of sector for short and long amplitudes of voltage vectors	26
3.9	Finalized voltage space vectors of 3-level Cascaded H-Bridge Multilevel	27
3.10	A de-couple control structure of DTC of induction machine using CHMI	29
3.11	Voltage vectors available in (a) 2-level inverter and (b) 3-level Cascaded H-Bridge Multilevel Inverter	32
3.12	Summarization on procedure to construct optimum look-up table for CHMI	33
4.1	Simulation result on Matlab of a de-couple control structure of DTC of induction machine	35
4.2	Performance comparison of torque control based on selection of vectors using (a) 2-level inverter (b) CHMI	37
4.3	Magnified simulation result obtain (a) 2-level inverter (b) CHMI	38
4.4	Switching frequency variation at 300 rpm (a) Conventional (V_{HZ}) (b) CHMI (V_{HL})	44
4.5	Switching frequency variation at 650 rpm (a) Conventional (V_{HZ}) (b) CHMI (V_{HL})	45
4.6	Switching frequency variation at 1000 rpm (a) Conventional (V_{HZ}) (b) CHMI (V_{HL})	46
4.7	Comparison the switching frequency at low speed operation. (a) Conventional inverter (b) zoom image of conventional inverter	

LIST OF FIGURES

FIGURE	TITLE	PAGE
	(c) CHMI (d) zoom image of CHMI	48
4.8	Comparison the switching frequency at medium speed operation. (a) Conventional inverter (b) zoom image of conventional inverter (c) CHMI (d) zoom image of CHMI	49
4.9	Comparison the switching frequency at high speed operation. (a) Conventional inverter (b) zoom image of conventional inverter (c) CHMI (d) zoom image of CHMI	49



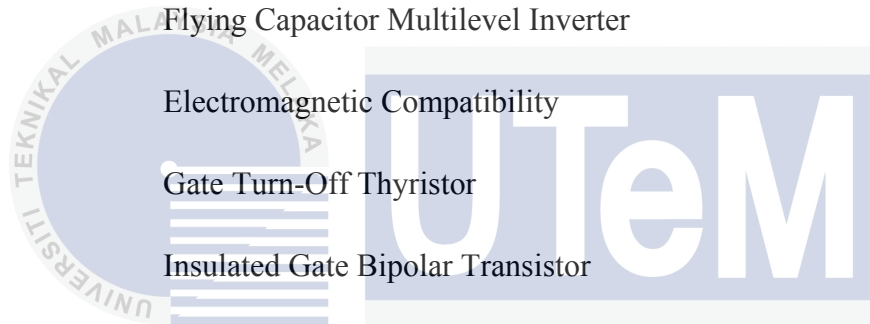
LIST OF APPENDICES

APPENDIX	TITLE	PAGE
A	Gantt chart	55



LIST OF ABBREVIATION

DTC	Direct Torque Control
FOC	Field Oriented Control
VSI	Voltage Sources Inverter
CHMI	Cascaded H-Bridge Multilevel Inverter
NPC	Neutral Point Clamped
FCMI	Flying Capacitor Multilevel Inverter
EMC	Electromagnetic Compatibility
GTO	Gate Turn-Off Thyristor
IGBT	Insulated Gate Bipolar Transistor



اونيورسيتي تيكنيكل مليسيا ملاك

UNIVERSITI TEKNIKAL MALAYSIA MELAKA

CHAPTER 1

INTRODUCTION

1.1 Overview

In the real industry world, control of induction machine play a vital role as it has many application in real work place. Induction machine has several advantages such as rugged, less complex and affordable in price. Direct torque control (DTC) is a vector based control technique that proposed in early 1980 where it involves the combination control of torque and flux by feedback and closed loop estimation process. A comprehensive researches and latest update based on this control technique has been proved by hundreds of paper related to this DTC are published since the last two decade. Furthermore, DTC only required information of resistance in stator which make it simpler control technique compared to field oriented control (FOC) which required both stator and rotor parameters. Nowadays, development of multilevel inverter recently has been a solution to the major problem highlighted in conventional inverter since it provides more effective voltage selection. For instance, cascaded H-Bridge multilevel inverter (CHMI), neutral point clamped (NPC) and flying capacitor multilevel inverter (FCMI) are among the three multilevel inverters that popular and many research related this have been publish. This is because the advantages that highlighted by multilevel inverter such as ability to achieve high power from medium source, can generate the output voltages with very low distortion and reduce the rate of change of voltage (dv/dt) which improve the electromagnetic compatibility (EMC) problem.

1.2 Project motivation

DTC technique that proposed using conventional inverter has several disadvantages such as less selection of effective voltage vector hence lead to high switching frequency. The limited voltage vectors selection are as shown in Figure 1.1 which comprise of six voltage amplitude. Less effective voltage vector happen because the fixed of two level in the conventional inverter has cause inappropriate selection of switching occur especially when changes of the speed happen. The high rate change of voltage (dv/dt) has cause increase in torque ripple [1]. By this improper selection of switch also lead to the increase in switching frequency. High switching frequency has cause losses to the operation of induction machine and increase possibility of overshoot to happen [1].

Therefore, by replacing the conventional inverter with the CHMI it bring significant improvement since the level of effective voltage has increase and lead to more strategy switching state during changes of speed occurs. By having proper selection of effective voltage vector, the torque ripple reduces [1]. Therefore, the efficiency of direct torque control of induction machine improves by the minimization of torque ripple since the switching frequency of inverter is also reduces.

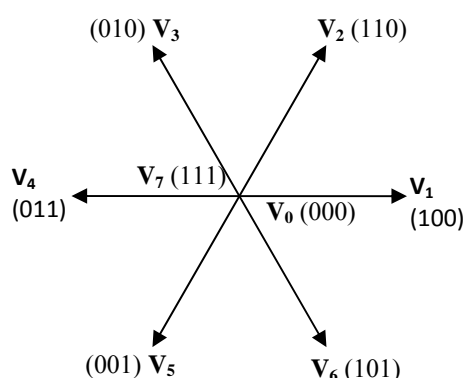


Figure 1.1: Limited voltage vector in conventional inverter lead to inappropriate selection of switching occurs

1.3 Objective

- (i) To formulate an optimal voltage vector selection according to speed operations for DTC of induction machine.
- (ii) To verify the proposed selection of voltage vectors can improve efficiency and reduce torque ripple.

1.4 Scope of research

The scope of this project focuses on the development of optimal look-up table for DTC utilizing on 3-level CHMI by using simulation only. The simulation was carried out using Matlab/Simulink simulation package. The simulation is then verified by adding switching frequency algorithm to the DTC simulation to carry the analysis. Comparison between 3-level CHMI and conventional inverter will be discussed after the final result is achieved to highlight the advantages of 3-level CHMI.

1.5 Report outline

The general description of this report outline is discussed in this subsection. Basically these reports are based on five chapters. The executive summary was provided before the first chapter to give overview of the whole project.

First and foremost, chapter one provides overview to give better understanding of the project. This chapter also highlights the significant of the problem statement, objective and scope of the project.

The second chapter provides information based on the conventional and basic topology of the project. The previous works based on the previous research will be discussed in detail to provide guideline to construct the next chapter.

Chapter three will discuss and highlight the method that use to model and construct the simulation. The result will be proving in the chapter four where it based on the work done in previous chapter.

Last but not least, conclusion section provide summary of the whole project. Recommendations based on the finding during the project also will be emphasize for the improvement on next project.

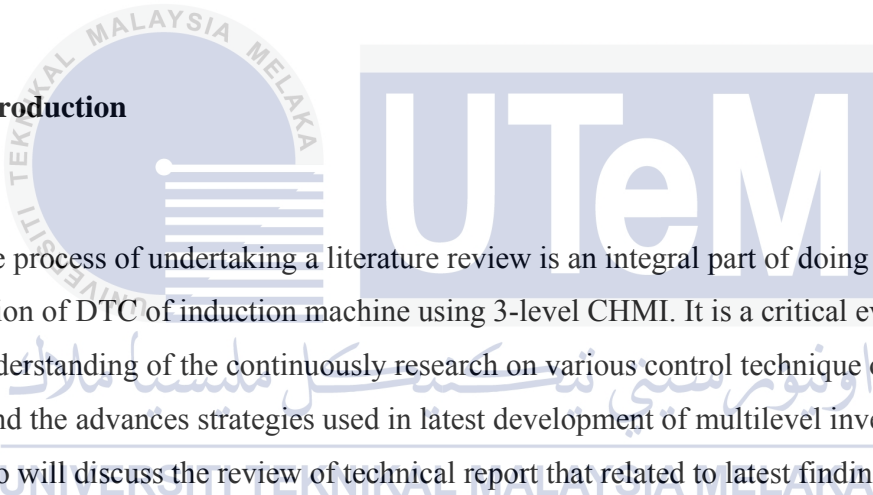


CHAPTER 2

LITERATURE REVIEW

2.1 Theory

2.1.1 Introduction



The process of undertaking a literature review is an integral part of doing this project on simulation of DTC of induction machine using 3-level CHMI. It is a critical evaluation to gain an understanding of the continuously research on various control technique of induction machine and the advances strategies used in latest development of multilevel inverter. This section also will discuss the review of technical report that related to latest finding in DTC and CHMI. Thus provides a clear, better and deeper understanding on technique to improve dynamic performance in correspond to compare the performance with conventional finding.

2.1.2 Control technique

Generally the control techniques to control speed of induction motor are based on scalar and vector control. Firstly, scalar controls proposed less complex technique to working with and bid better steady-state response. However, the dynamic response take long times since the transient are uncontrollable. Frequency of voltage and current is the parameter to be controlled in scalar. Early in 1970, to control induction machine, the field oriented control which emphasize on the principle of torque and flux control was introduced. Later on, a decade after, DTC was proposed. Figure 2.1 summarized the flowchart of variable frequency control. The highlight part to indicate the focuses of this project that is DTC.

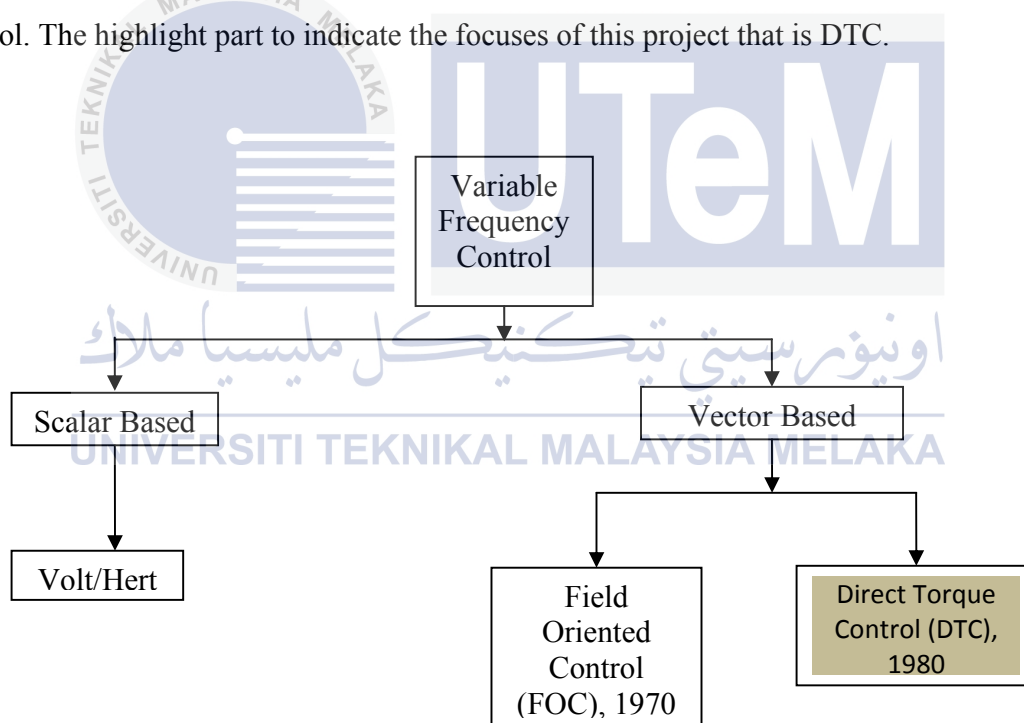


Figure 2.1: Summarization on the evolution of control technique scheme

2.1.3 Conventional three phase voltage source inverter (VSI)

This subsection provides a review about conventional three phase two level inverter. Inverter function basically is to convert direct current (DC) to alternating current (AC). Figure 2.2 shows three phase VSI that contain six numbers of insulated gate bipolar transistor (IGBTs) or gate turn-off thyristor (GTOs) where each leg made up of a pair power switching devices. This power switching devices is complimentary to one another on operation. For instance, when voltage is supply to the IGBTs, if upper switch (S_{a1}) is ON the lower switch (S_{a2}) must be OFF and vice versa.

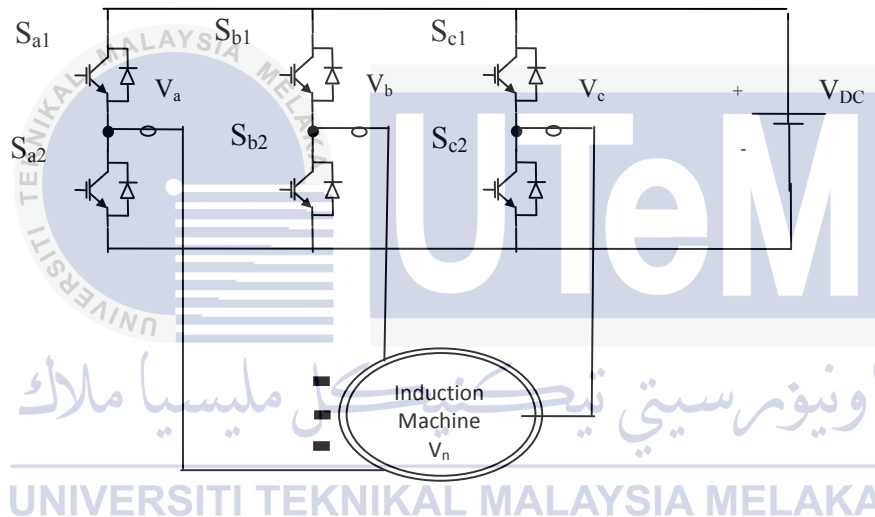


Figure 2.2: Topology of Voltage Sources Inverter (VSI)

In general, the switching state can have 8 different possibilities of switching from the equation 2^n where $n=3$ are the number of legs contain in VSI. The possibilities are show in Figure 2.3 based on type of voltage vector plotted by the given equation [2.1]

$$V_k = \frac{2}{3} V_{DC} (S_a + aS_b + a^2S_c) \quad \text{where } a = e^{j2\pi/3} \text{ and } k = 0, 1, 2 \dots 7. \quad (2.1)$$

where V_k is the different possibilities of switching in voltage space vector

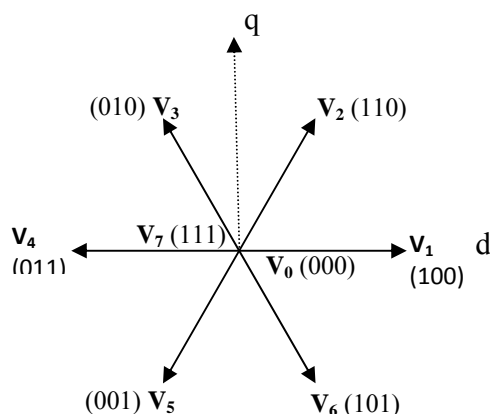


Figure 2.3: Voltage space vectors of a 3-phase inverter with the corresponded switching states

2.1.4 Basic principle in direct torque control (DTC)

In order to construct a look-up table, the basic principle in general must be followed to ensure all the requirement parameter included in this part. Three important parameter in this part is flux error status, torque error status and sector definition. Firstly, direct flux control are as shown in Figure 2.4 where the flux error enter the two level hysteresis comparator to produce flux error status φ^+ either 0 or 1. The error is obtaining by comparing the reference input flux, $\varphi_{s, \text{ref}}$ and estimated stator flux, φ_s . The summary of this process are highlighted in Figure 2.5.

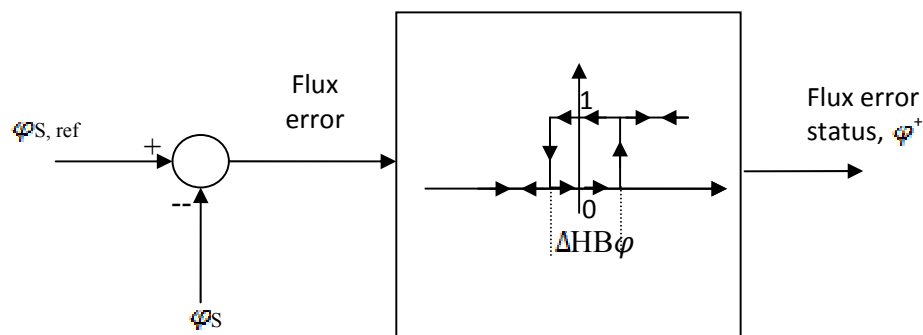


Figure 2.4 Control of flux magnitude using a 2-level hysteresis comparator

Flux error status	$\left\{ \begin{array}{l} 1 \\ 0 \end{array} \right.$	1 Touches lower band, stator flux need to be decrease
		0 Touches upper band, stator flux need to be increase

Figure 2.5: Summary of flux error status in hysteresis band

Beside flux, torque also needs to be controlled. Secondly, DTC are as shown in Figure 2.6 where the torque error enter the three level hysteresis comparator to produce torque error status, T_{stat} either 1,0 or -1. The errors are obtained by comparing the reference input torque, $T_{e,ref}$ and estimated torque flux, T_e . The summary of this process are highlighted in Figure 2.7.

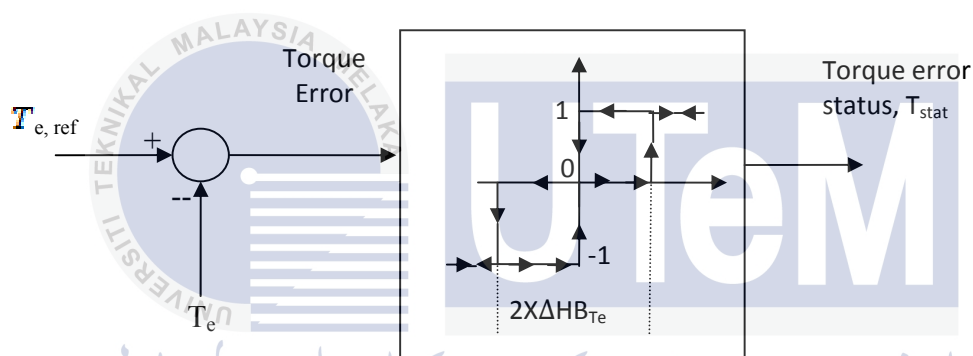


Figure 2.6: Control of torque using a 3-level hysteresis comparator

Torque error status	$\left\{ \begin{array}{l} 1 \\ 0 \\ -1 \end{array} \right.$	1 Touches upper band, active forward voltage vector
		0 Touches middle band, zero voltage vector selected
		-1 Touches lower band, active reverse voltage vector

Figure 2.7: Summary of torque error status in hysteresis band

Last but not least are the sector definitions, which are divided equally to six sectors. For example, Figure 2.8 illustrates on how the flux is increased and decreased with the use of voltage vectors V_1 and V_2 respectively when it lies in Sector II. This pattern continuous for one completes cycle with the pattern increase and decrease by the use of different voltage vector.

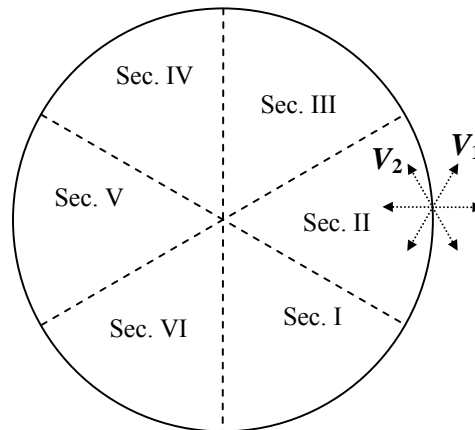


Figure 2.8: Definition of six sectors of the stator flux plane

After all the three parameters are gather, the voltage vector selection table are produce also known as look-up table as show in Table 2.1. The output of this look-up table later will fed into 3-level CHMI later on and also used for voltage calculation of V_d and V_q .

Table 2.1: Voltage vector selection table [2]

Stator flux error status, Ψ_s^+	Torque error status, T_{stat}	Sector I	Sector II	Sector III	Sector IV	Sector V	Sector VI
1	1	[100]	[110]	[010]	[011]	[001]	[101]
	0	[000]	[111]	[000]	[111]	[000]	[111]
	-1	[001]	[101]	[100]	[110]	[010]	[011]
0	1	[110]	[010]	[011]	[001]	[101]	[100]
	0	[111]	[000]	[111]	[000]	[111]	[000]
	-1	[011]	[001]	[101]	[100]	[110]	[010]

The selection of suitable switching state are obtain as shown in Table 2.1 based on necessity either to increase or decrease flux and torque respectively and also based on sector definition. The overall topology on de-couple structure of DTC-hysteresis based on the induction machine are as shown in Figure 2.9.

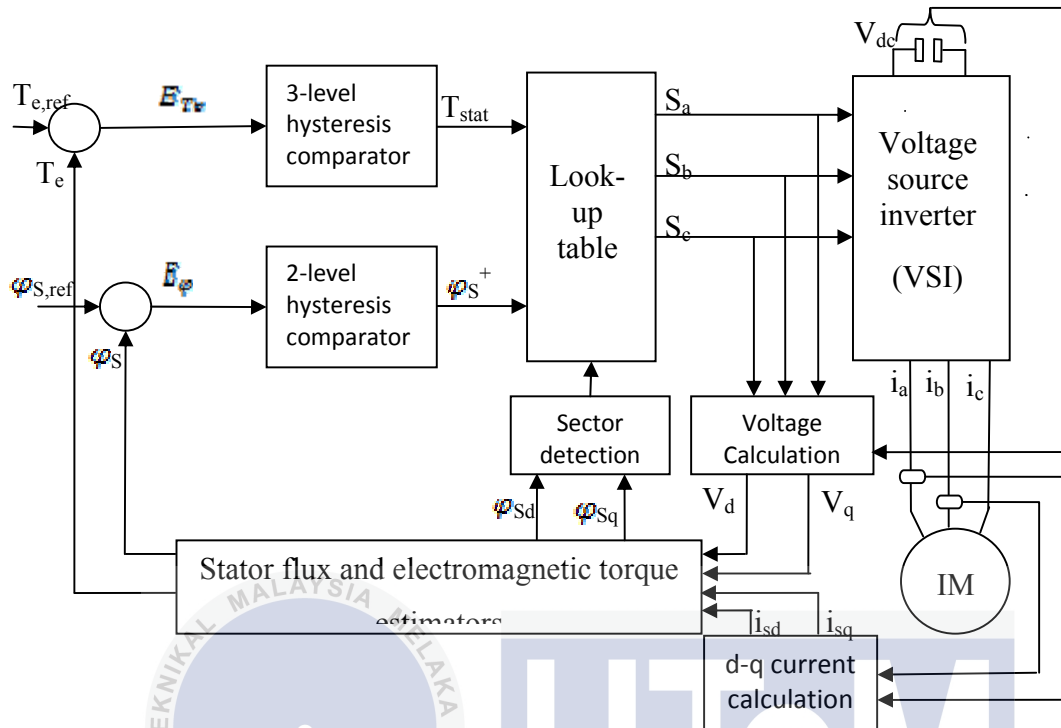


Figure 2.9: A conventional control structure of DTC-hysteresis based induction machine [2]

2.1.5 Types of multilevel inverters

In the previous part, the topology of conventional inverter has highlighted. This part will review the important of multilevel inverter. Besides able to withstand on high voltage, multilevel inverter has many advantages compared to conventional such as low dv/dt make multilevel inverter are the better choice. The understanding that related to the multilevel converters has been introduced since 1891 where the novel structure was proposed in [2]. Among the advantages that highlight in [3] are the less harmonic contain by compared the result with conventional two level inverters. However, there are several disadvantages highlighted that is their complexity, increasing number in switching devices and complex control circuitry [4].

Three types of multilevel inverter that will be discussed and to be understood in this literature review is neutral point clamped (NPC) or diode clamped multilevel inverter, flying

capacitor or capacitor clamped multilevel inverter and cascaded H-bridge multilevel inverters (CHMI) [5]. Since this project focuses the DTC of induction machine based on 3-level CHMI, hence detail and comprehensive studies on this topology will be emphasized. Otherwise the neutral point clamped and flying capacitor will be discussed in general.

2.5.1.1 Neutral Point Clamped (NPC)

The neutral point clamped (NPC) also known as diode clamped multilevel inverter was proposed in [6]. The topology of this NPC is based on twelve power semiconductor switches (IGBTs) which divide into three legs respectively. Each leg is clamped in parallel with two series connected diode. A capacitor was placed parallel to the sources. Another two capacitors are halved and connected in series to form a neutral point N which means three total number of capacitor are used in this 3-level NPC [5]. Figure 2.10 shows the topology of 3-level NPC which in these configuration two power switches conduct simultaneously.

However there are unbalanced DC-link voltage problem related to NPC. A simple control strategy based on the discontinuous pulse width modulation method (DPWM) is proposed. The DPWM method is used to balance the DC-link voltage in the three-level inverter. By these strategies, it can be effectively balanced without complicated calculation or an additional balancing circuit and verify by experiment in [7].

In term of DTC scheme using NPC, the result obtained show that improvement in term of dynamic performance compared with 2-level inverter by lower torque ripple state in [8]. This paper also mention the proper switching vector in multilevel application compared to the conventional inverter. In conventional, the torque and flux ripples are higher because the switching vectors choose for large errors are the same as for small errors.

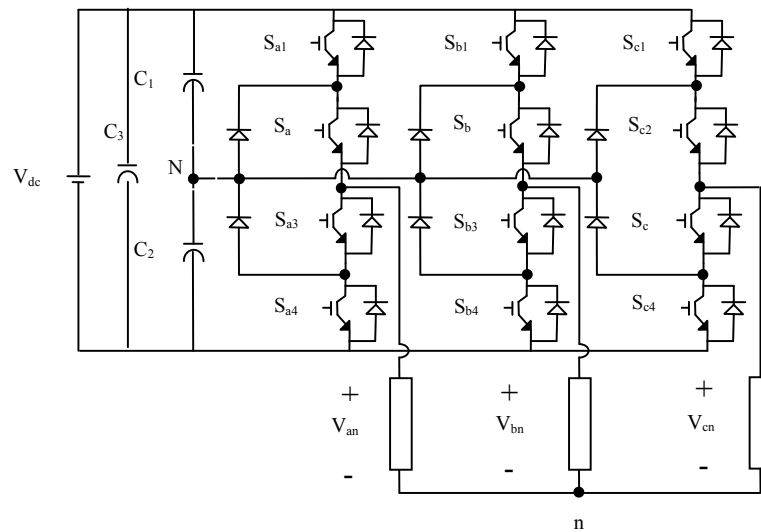


Figure 2.10: Three phase three level of neutral point clamped

2.5.1.2 Flying Capacitor Types Multilevel Inverters (FCMI)

The flying capacitor also known as capacitor clamped multilevel inverter. Figures 2.11 shows topology of FCMI which consist of twelve power semiconductor switches (IGBTs) divide into three legs respectively. Each leg is clamped in parallel with single capacitor. On the other hand, one capacitor is set parallel with sources, and another 2 was connected to neutral. Thus, six total number of capacitor are used in this three-level FCMI.

Problem related to this FCMI such as output current changes the voltage of the capacitors and the excitation of the inverter is special. The flying capacitor required charged of clamping in order to start [4].

In recent research for renewable energy using photovoltaic (PV), a new topology of FCMI is proposed in [4] by a capacitor clamped DC–DC boost converter used in order to overcome harmonic. The proposed seven-level FCMI in [9] not only achieves high power ratings, but also enables the use of renewable energy sources in an efficient manner.

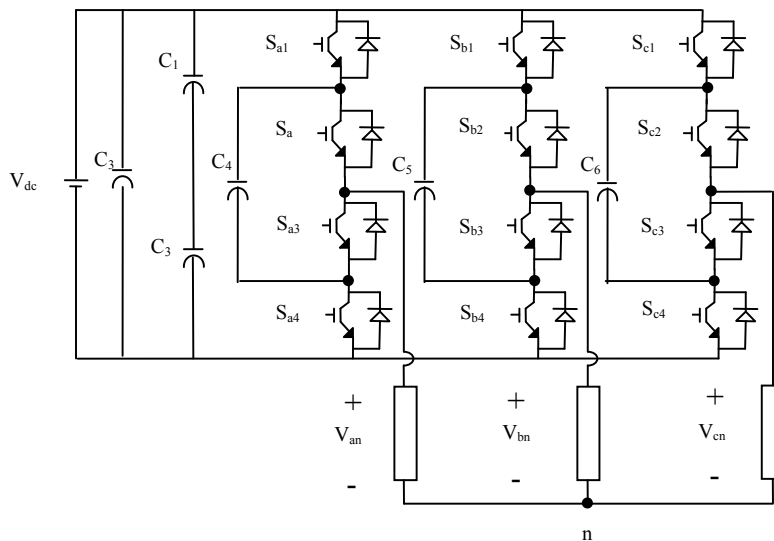


Figure 2.11: Three phase three level flying capacitor multilevel inverter

2.5.1.3 Cascaded H-Bridge Multilevel Inverter (CHMI)

A 3-level CHMI contains twelve numbers of power switching devices. It made of three phases where in each phase the H-bridge inverter is supply with separated DC source. It can be noticed that the representation of each switching state is complementary to each other. Figure 2.12 show the topology of three phase 3L-CHMI. Recently, a new method present by using multilevel DC link (MLDCL) and a bridge inverter to reduced the number of switching as shown in [10]. This topology can have enhanced performance by implementing the pulse width modulation (PWM) techniques.

Besides that, a proposed CHMI consists of one single dc input source and several low-frequency three phase transformer highlight in [11]. The advantages of using this isolated CHMI, is the reduction of cost. New topology of multilevel inverters has proposed in [12] which have the advantages of reducing the number of device. Analysis done in this finding also highlights the reduction in harmonic distortion.

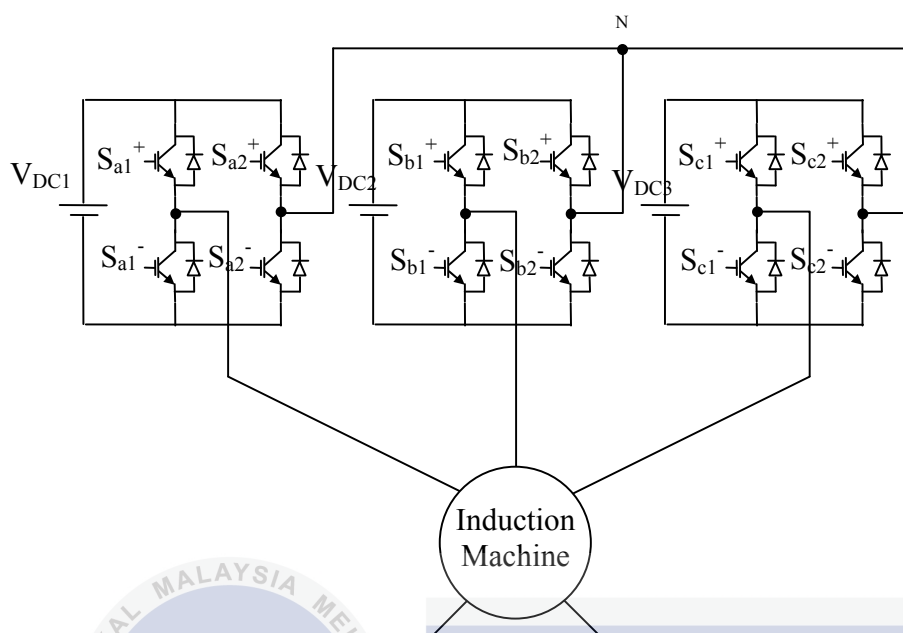


Figure 2.12: Three levels CHMI connected to 3-phase induction machine.

2.1.6 Inverter performance analysis

This section reviews the analysis that done by researcher in order to prove the finding of multilevel inverter is much better compared to the conventional inverter. The analysis had done include the waveform pattern, harmonic spectrum, fundamental value and total harmonic distortion [13, 14]. The effects of hysteresis controllers on the performance of DTC also study in order to help researcher to have the best bandwidth setting at the comparator. The performance of inverter also depends on the different speed setting at the induction machine [14].

2.2 Related previous work

In 1986, a group of researches lead by Takashi proposed a vector based control method by combination of flux and torque known as direct torque control (DTC) [2]. Based on this control mechanism, many researchers have been done within this three decade. Generally the

concepts of DTC are based on parameter at the stator, voltage and current quantities. This parameter is important and required in order to estimate flux and torque. The differences of DTC and another famous vector control that is field oriented control (FOC) have been discussed in [1], [15] and [16] to compare their basic topology and dynamic performance.

In order to obtain a fast dynamic torque response in DTC, novel overmodulation, simple overmodulation and overmodulation strategy methods are proposed [17][18] and [19]. Dynamic overmodulation method is one of the solutions that modified flux error before fed into look-up table [20] and [21]. This is done by increase the voltage limit which increases the torque region. The overmodulation is use to extend the constant torque region which produce high torque capability in field weakening region by using VSI. This overmodulation technique is discussed in detail in [18-21].

Implementation DTC on the multilevel inverter has influent many researchers all around the world to study the problem arise related to this control mechanism. Latest control on multilevel inverter is done by replacement of VSI to a multilevel inverter structure such as CHMI, NPC and FCMI state in [8] and [22]. Advanced research studies the performance of DTC based on CHMI on the automatic application [9] where it provides high efficiency, and reduce switching losses. Researches on reduce the torque ripple and implementation of fuzzy logic in CHMI are discuss in [10]. Basically they are tremendous number of research on direct torque control using multilevel inverter but by picking relevant important study this previous work were construct. The improvement in performance of DTC using CHMI in term of torque ripple and quality of total harmonic distortion are highlighted in [1], [13] and [15].

2.3 Summary of review

Based on the background of this project that discuss in this section, it give insights into the content of a proposed title. Literature review provides coherent argument that comes from the previous researcher. By know all the basic topology that related previous work, it give confident to develop idea on the next chapter outlines hence implement it.

CHAPTER 3

METHODOLOGY

3.1 Research Methodology

3.1.1 Introduction

This section will discuss the method used in order to model the simulation for DTC of induction machine using 3-level CHMI. A comprehensive investigation of DTC variations method based on the reading of current technical papers and journal is necessary in order to construct the simulation model. This investigation will emphasize on the topics of DTC utilizing on multilevel inverter. The literature reviews on previous works are discussed previously in Chapter 2. The rest procedures to model the simulation are given in this section.

3.1.2 Mathematical model of induction machine

The induction machine models in the general reference frame with iron loss consideration are expressed as follows in [3.1], [3.2], [3.3], [3.4] and [3.5]:

$$V_s = R_s I_s + (d\varphi_s/dt) \quad (3.1)$$

$$0 = R_r I_r - j\omega_r \varphi_r + (d\varphi_r/dt) \quad (3.2)$$

$$\varphi_s = L_s I_s + L_m I_r \quad (3.3)$$

$$\varphi_r = L_r I_r + L_m I_s \quad (3.4)$$

$$T_e = \frac{3}{2} P |\varphi_s| |I_s| \sin \delta \quad (3.5)$$

Where P is the number of pole pairs, ω_r is the rotor electric angular speed in rad/s, L_s , L_r and L_m are the motor inductance, R_s is the stator resistance and R_r is the rotor resistance.

3.1.3 Three phase 3-Level Cascaded H-Bridge Multilevel Inverter topology

A 3-level CHMI contains six power switching devices for upper leg and lower leg respectively. This topology composed of three phases where in each phase the H-bridge inverter is supply by independent DC source. Figure 3.1 shows the simplified version of 3-level CHMI that connected to induction machine. It can be notice that the representation of each switching state is complementary to each other. This means the switching state of each phase $[S_{a1}, S_{a2}]$, $[S_{b1}, S_{b2}]$ and $[S_{c1}, S_{c2}]$ equal to 1 when the upper leg is ON and 0 when the lower switch is OFF and vice versa. Note that Figure 3.1 shows individual H-bridge inverter configuration consist of two pairs power switching on 2 leg respectively. It is impossible for both upper switching devices in each phase ON at the same time. It can be shown the inverter phase voltage for each phase can be written as [3.6], [3.7] and [3.8]:

$$V_{aN} = V_{dc}(S_{a1} - S_{a2}) \quad (3.6)$$

$$V_{bN} = V_{dc}(S_{b1} - S_{b2}) \quad (3.7)$$

$$V_{cN} = V_{dc}(S_{c1} - S_{c2}) \quad (3.8)$$

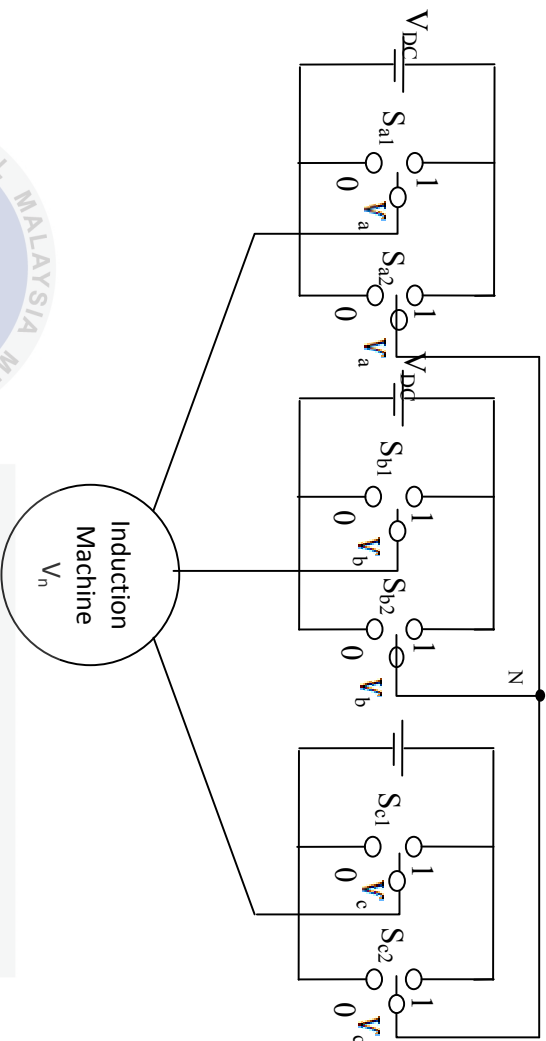


Figure 3.1: Simplified topology 3 Level Cascaded H-bridge Multilevel Inverter connected to 3-phase Induction machine.

Based on Table 3.1, it can be shown that the total combination of switching state in three phase 3-level CHMI is sixty four, ($2^6 = 64$) but based on the possibility switching condition of H-bridge configuration discuss in the earlier part only 27 voltage space vectors are choose out of 64 switching state. On the other hand, 37 combinations that show possibility for both switches that is either $[S_{a1}, S_{a2}]$, $[S_{b1}, S_{b2}]$ nor $[S_{c1}, S_{c2}]$ in each phase on at the same time are rejected. Details of this selection are shown in Table 3.1 which provides the information of rejected switching possibility. For example, if number 3 is chosen, the possibility is 000011 which means $[S_{c1}, S_{c2}]$ need to be on at the same time that is impossible hence this possibility is rejected. This impossibility condition part was highlighted by red color in the Table 3.1 which indicate reject.

No.	Switching state	Direction	Description
-----	-----------------	-----------	-------------

possible	S _{a1}	S _{a2}	S _{b1}	S _{b2}	S _{c1}	S _{c2}	LEFT	RIGHT	
1	0	0	0	0	0	0		0	ZERO
2	0	0	0	0	0	1		↗	SHORT
3	0	0	0	0	1	0	↙		SHORT
4	0	0	0	0	1	1			REJECT
5	0	0	0	1	0	0		↘	SHORT
6	0	0	0	1	0	1	→		SHORT
7	0	0	0	1	1	0		↓	MEDIUM
8	0	0	0	1	1	1			REJECT
9	0	0	1	0	0	0	↙		SHORT
10	0	0	1	0	0	1		↑	MEDIUM
11	0	0	1	0	1	0		←	SHORT
12	0	0	1	0	1	1			REJECT
13	0	0	1	1	0	0			REJECT
14	0	0	1	1	0	1			REJECT
15	0	0	1	1	1	0			REJECT
16	0	0	1	1	1	1			REJECT
17	0	1	0	0	0	0		←	SHORT
18	0	1	0	0	0	1	↗		SHORT
19	0	1	0	0	1	0	↘		MEDIUM
20	0	1	0	0	1	1			REJECT
21	0	1	0	1	0	0	↙		SHORT
22	0	1	0	1	0	1		0	ZERO
23	0	1	0	1	1	0	↙		LONG
24	0	1	0	1	1	1			REJECT
25	0	1	1	0	0	0	↙		MEDIUM
26	0	1	1	0	0	1	↘		LONG
27	0	1	1	0	1	0		←	LONG
28	0	1	1	0	1	1			REJECT
29	0	1	1	1	0	0			REJECT
30	0	1	1	1	0	1			REJECT
31	0	1	1	1	1	0			REJECT
32	0	1	1	1	1	1			REJECT
33	1	0	0	0	0	0	→		SHORT
34	1	0	0	0	0	1		↗	MEDIUM
35	1	0	0	0	1	0		↘	SHORT
36	1	0	0	0	1	1			REJECT
37	1	0	0	1	0	0		↘	MEDIUM
38	1	0	0	1	0	1	→		LONG
39	1	0	0	1	1	0		↘	LONG
40	1	0	0	1	1	1			REJECT
41	1	0	1	0	0	0		↗	SHORT
42	1	0	1	0	0	1		↘	LONG
43	1	0	1	0	1	0		0	ZERO
44	1	0	1	0	1	1			REJECT
45	1	0	1	1	0	0			REJECT
46	1	0	1	1	0	1			REJECT
47	1	0	1	1	0	1			REJECT
48	1	0	1	1	1	1			REJECT
49	1	1	0	0	0	0			REJECT
50	1	1	0	0	0	1			REJECT
51	1	1	0	0	1	0			REJECT
52	1	1	0	0	1	1			REJECT
53	1	1	0	1	0	0			REJECT
54	1	1	0	1	0	1			REJECT
55	1	1	0	1	1	0			REJECT
56	1	1	0	1	1	1			REJECT
57	1	1	1	0	0	0			REJECT
58	1	1	1	0	0	1			REJECT
59	1	1	1	0	1	0			REJECT
60	1	1	1	0	1	1			REJECT
61	1	1	1	1	0	0			REJECT
62	1	1	1	1	0	1			REJECT
63	1	1	1	1	1	0			REJECT
64	1	1	1	1	1	1			REJECT

Reject: Possibility of both switch on the same leg on at the same time

In general, the phase voltage space vectors of the 3-level CHMI for every possibility switching state express by the following equation [3.9]:

$$V^* = V_d + jV_q \quad (3.9)$$

Where V_d and V_q are given as follow in [3.10] and [3.11]

$$V_d = \frac{V_{dc}}{3} (2S_{a1} - 2S_{a2} - S_{b1} + S_{b2} - S_{c1} + S_{c2}) \quad (3.10)$$

$$V_q = \frac{V_{dc}}{\sqrt{3}} (S_{b1} - S_{b2} - S_{c1} + S_{c2}) \quad (3.11)$$

Note that the d-axis and q-axis voltage original equation are obtained from [3.12] and [3.13]:

$$V_d = \frac{1}{3} (2V_{aN} - V_{bN} - V_{cN}) \quad (3.12)$$

$$V_q = \frac{1}{\sqrt{3}} (V_{bN} - V_{cN}) \quad (3.13)$$

3.2 Analytical Approach

3.2.1 Design of look-up table for 3-level CHMI

In order to construct the look-up table, it is important to understand the three parameter mention in previous chapter. The flux magnitude was control by 2-level hysteresis comparator while the torque using 7-level hysteresis comparator. The control for flux has discussed earlier in chapter 2 based on mechanism show in Figure 2.4 and the summarization of flux error status was given in Figure 2.5. When the error touches it upper or lower hysteresis band, an appropriate voltage vector is selected to reduce or to increase it respectively. The hysteresis comparator will produce flux error status which can be either 1 or 0 as in Figure 2.5. The typical waveform in Figure 3.2 is to illustrate the mechanism that happens in Figure 2.4.

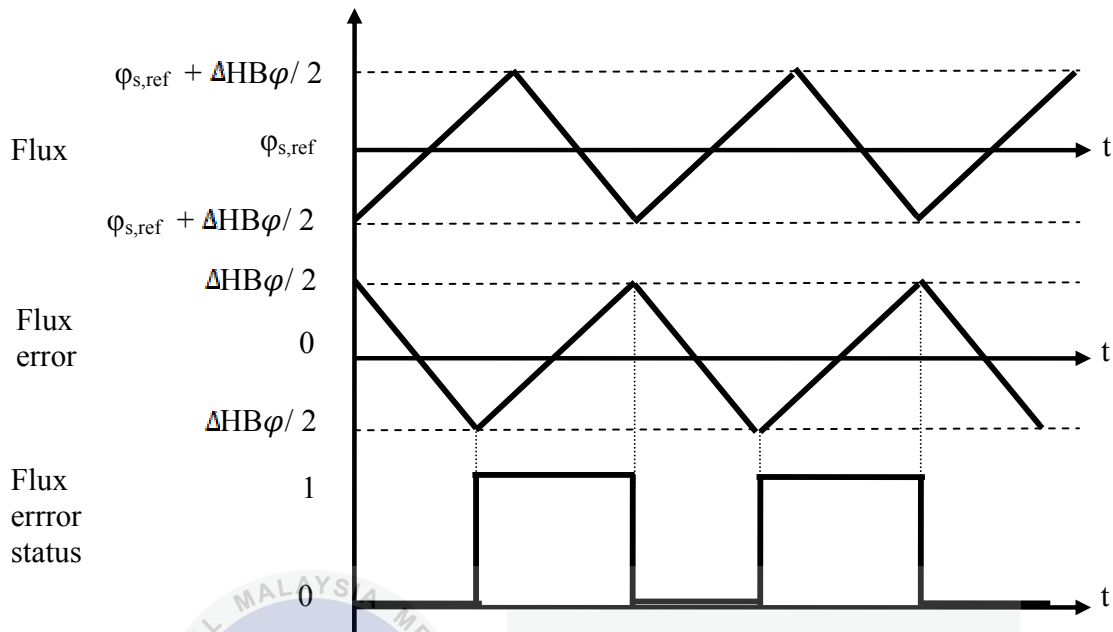


Figure 3.2: Typical waveform of the flux, the flux error and the flux error status for the two-level hysteresis torque comparator

After neglected the ohmic drop voltage over small period of time the space vectors in the stator voltage equation is given by equation (3.14). This equation defined that the stator voltage space vector controls the stator flux linkage directly.

$$\Delta\varphi_s = v_s \Delta t \quad (3.14)$$

where, φ_s represent variation of stator flux linkage, v_s represent stator voltage space vector and t represent time.

Besides 2-level hysteresis comparator, a 7-level hysteresis comparator is necessity in torque controlling. By increase the level of comparator it actually signifies the more levels of error. The controlling mechanism of torque are as shown in Figure 3.3 where the torque error enter 7-level comparator to produce torque error status, T_{stat} either 3,2,1,0,-1,-2 or -3. By comparing the references input, $T_{e,ref}$ and actual torque, T_e , the torque error status can be determined. Figure 3.4 summarized the significant of each level in controlling torque using 7-level comparator. Figure 3.5 indicate the typical waveform of the torque using a 7 level comparator which show the proper selection of torque error status.

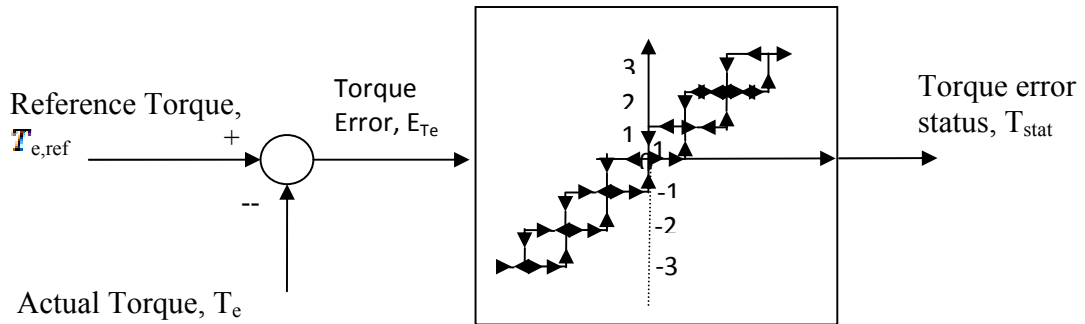


Figure 3.3: Control of torque using a 7-level hysteresis comparator

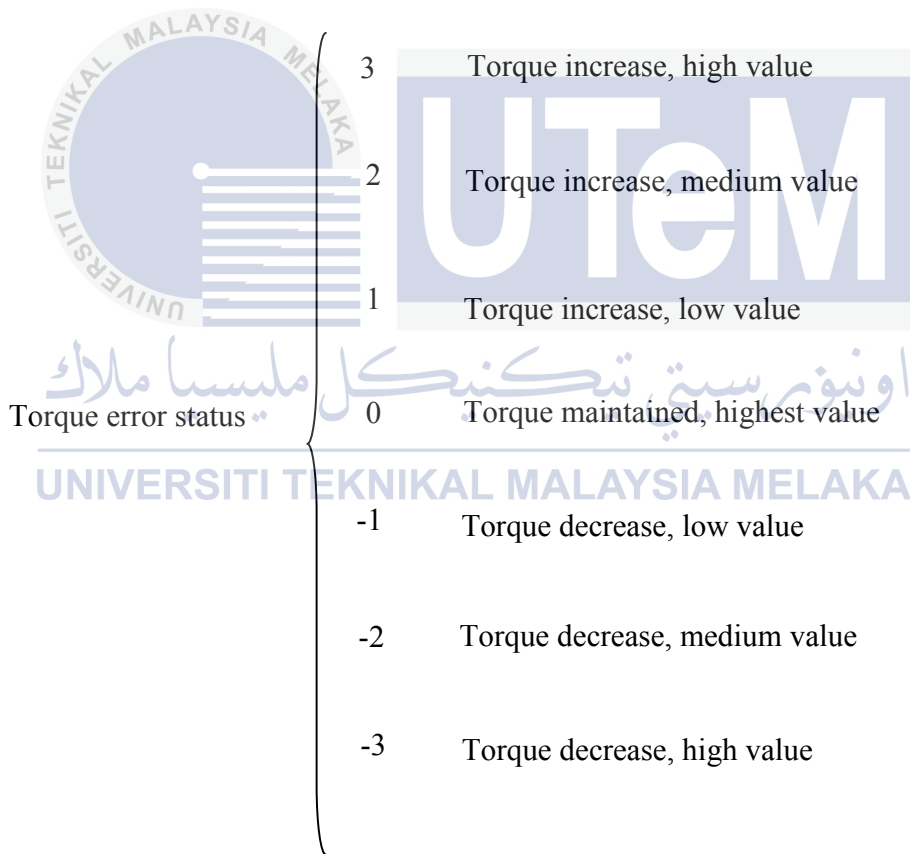


Figure 3.4: Summary of torque error status in hysteresis band

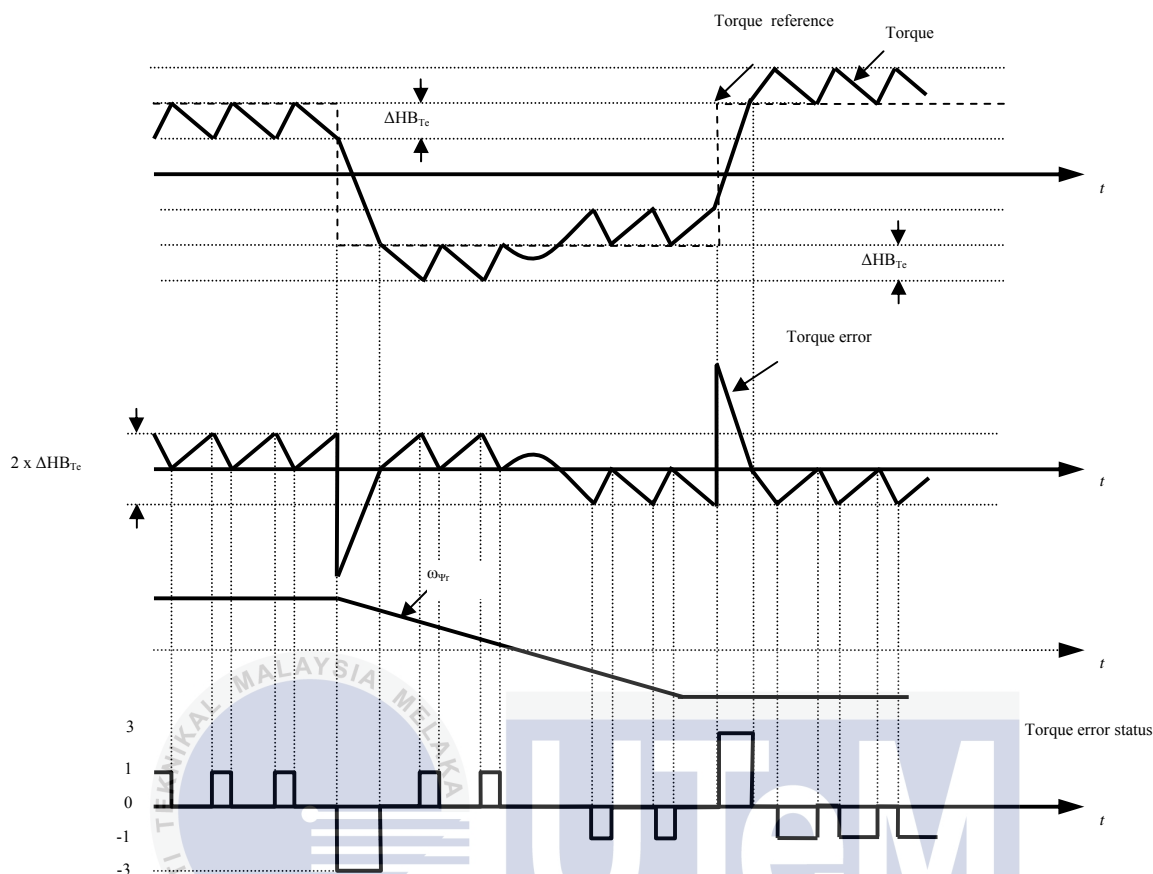


Figure 3.5: Typical waveform of the torque, the torque error and the torque error status for the seven-level hysteresis torque comparator

Last but not least is to define the sectors of the stator flux plane. By definition of each sector, the circular flux control for each sector can be performed using two possible active voltage vectors either to increase flux or decrease it. Figure 3.6 (a) and Figure 3.6 (b) give clearer step to select the optimal look-up table based on six sectors. For instance in Figure 3.6 and Figure 3.6 (a) show selection of V_1 is to indicate flux increase and V_2 to indicate flux decrease in sector III. For example related to long and short amplitude, the definition sector is in Figure 3.6 (a) and otherwise for medium refers to Figure 3.6 (b). Figure 3.7 provide the circular path reference by selecting appropriate voltage vector according to the flux positions. The path illustrate how the flux is increased and decreased with the usage of voltage vector in sector I and sector II. For instance in sector I, in order for the flux to increase it will choose V_2 and to decrease it will choose V_3 .

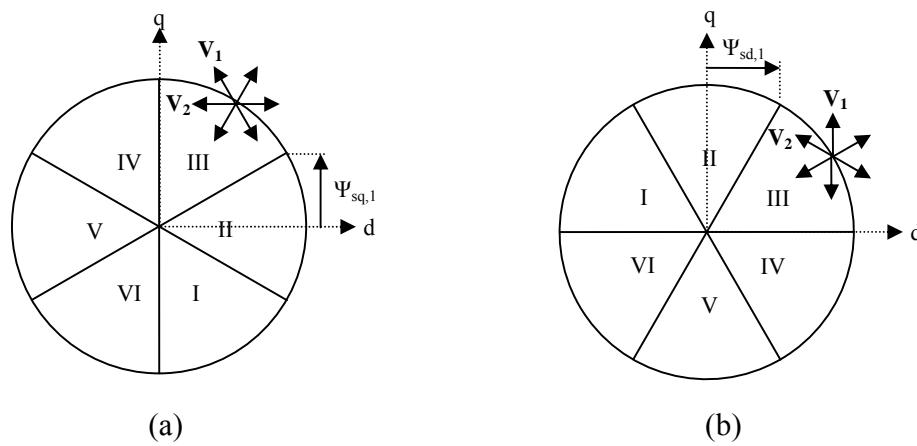


Figure 3.6: The sector definition of (a) the stator flux plane for long and short voltage vector
(b) the stator flux plane for medium voltage vector

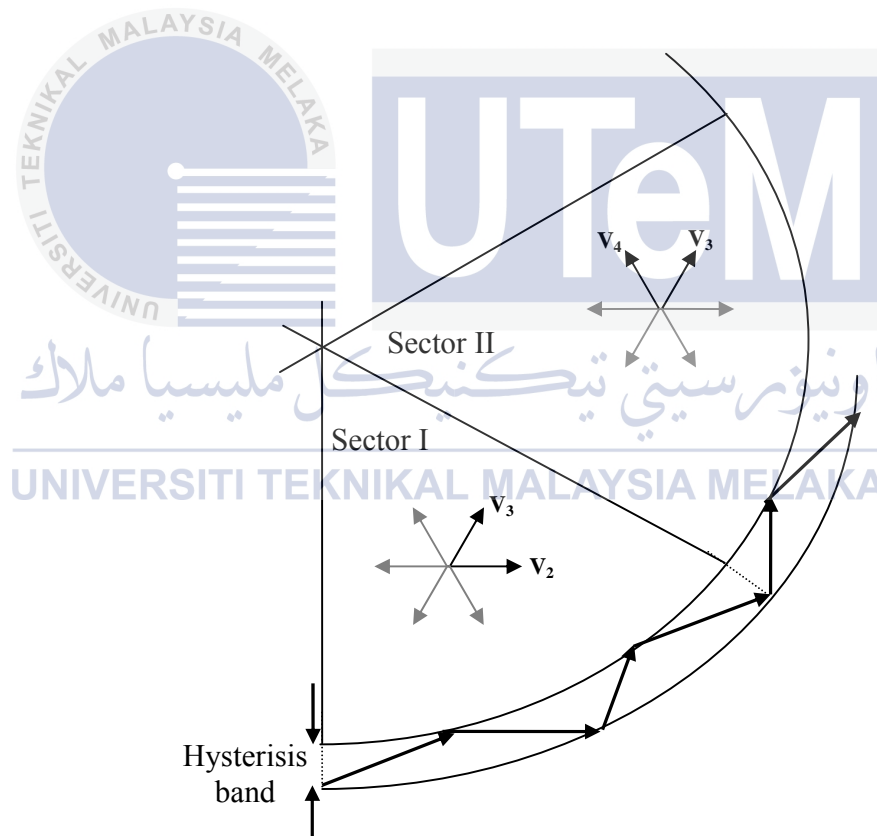


Figure 3.7: Two possible active voltage are switched for each sector to control the stator flux within its hysteresis band

The Figure 3.8 represents the whole sector definition for short, medium and long voltage vector. The highlighted flux is to determine the medium voltage vector which referred to the Figure 3.6 (a). Otherwise, to determine short and long amplitude voltage vector, Figure 3.6 (a) will be refer. This part will be represents in Matlab by the construction of coding in Input file to get 18 possibility sectors.

Sector identifying of stator flux based on the $\Psi_{sq,1}$ and $\Psi_{sd,1}$ can be simplified as shown in Figure 3.8. The $\Psi_{sq,1}$ is use to identify the sector for short and long amplitude voltage vector and $\Psi_{sd,1}$ is use to identify sector for medium amplitude voltage vector . For example, to determine sector 3 for medium voltage vector there are three steps must be followed. Firstly, the horizontal area must be at positive side of d (upper side). After that, it also must be at the positive side of vertical that is on the right hand side of q. Last but not least, by comparing between flux $\Psi_{sd,1}$ and Ψ_{sd} . If Ψ_{sd} is greater than $\Psi_{sd,1}$, sector III are obtain and otherwise sector II . Detail of the whole sector definition is representing in Figure 3.8.

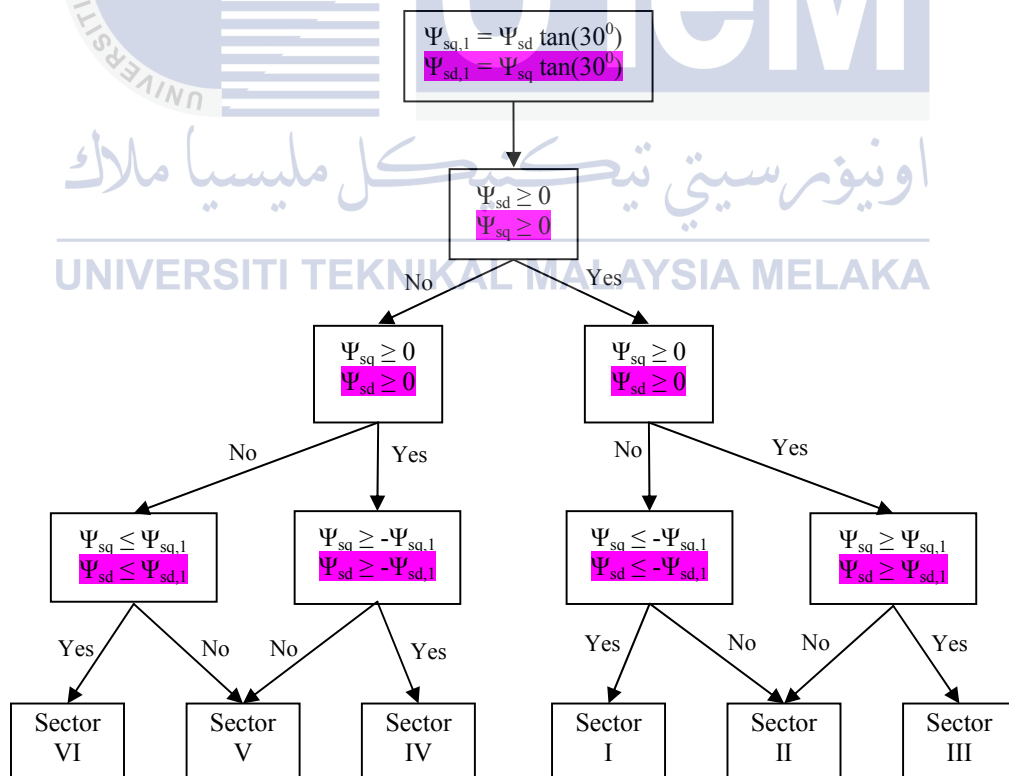


Figure 3.8: Definition of sector for short and long amplitudes of voltage vectors

Based on the Table 3.1, it can be summarized that the voltage direction on the table to obtain the voltage space vector as produced in Figure 3.9. Based on Figure 3.9, there is no problem for the long and medium voltage space vector determination but for short voltage space vector there must be only one possibility for switching instead of two. In order to overcome this problem, first compare the long voltage vector with the three possibilities at zero voltage vectors and choose the one that show minimum changes of bit. Later on, use the zero voltage vectors that selected earlier then compared with the short voltage space vector to get only single possibility of short voltage vector by taking the voltage vector that show minimum changes of switching state.

This process is repeated in order to produce single switching selection for all short voltage vectors. The results are shown as Figure 3.9 where the highlight switching state is chosen. From the voltage space vector constructed in 3-level CHMI it has twenty one possibilities of effective space voltage vectors which consist of three zero voltage vectors at the origin and eighteen non-zero voltage vectors. Focusing on the non-zero voltage vector it can be divided into 3 different groups based on long amplitude, medium amplitude and short amplitude voltage space vector.

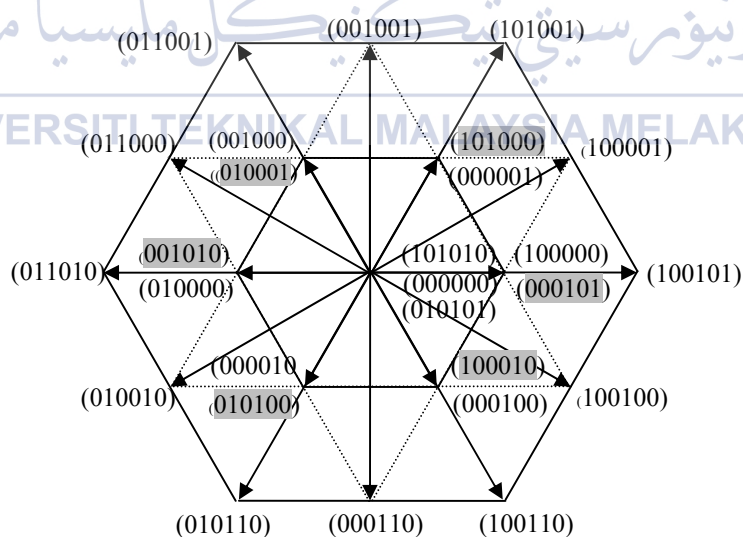


Figure 3.9: Finalized voltage space vectors of 3-level Cascaded H-Bridge Multilevel

Therefore by generating the voltage space vector it is easier to complete the look-up table. This table provides information of status flux error, ϕ_s^+ , torque error status, $T_{e,stat}$ and stator flux plane sector. In order to complete the table, circular flux control is applied on each sector in Figure 3.6 (a) and Figure 3.6 (b). The result is obtained as provided in Table 3.2.

Table 3.2: Voltage vectors selection table for 3-level CHM Inverter

Stator flux error status, ψ_{s^+}	Torque error status, T_{stat}	Sector I	Sector II	Sector III	Sector IV	Sector V	Sector VI
1	3	[100101]	[101001]	[011001]	[011010]	[010110]	[100110]
	2	[010010]	[011000]	[001001]	[100001]	[100100]	[000110]
	1	[000101]	[101000]	[010001]	[001010]	[010100]	[100010]
	0	[010101]	[101010]	[010101]	[101010]	[010101]	[101010]
	-1	[010100]	[100010]	[000101]	[101000]	[010001]	[001010]
	-2	[001001]	[100001]	[100100]	[000110]	[010010]	[011000]
	-3	[010110]	[100110]	[100101]	[101001]	[010001]	[011010]
	3	[101001]	[011001]	[011010]	[010110]	[100110]	[100101]
	2	[000110]	[010010]	[011000]	[001001]	[100001]	[100100]
0	1	[101000]	[010001]	[001010]	[010100]	[100010]	[000101]
	0	[101010]	[010101]	[101010]	[010101]	[101010]	[010101]
	-1	[001010]	[010100]	[100010]	[000101]	[101000]	[010001]
	-2	[100001]	[100100]	[000110]	[010010]	[011000]	[001001]
	-3	[011010]	[010110]	[100110]	[100101]	[010101]	[011001]

3.2.2 Stator flux and torque estimator

This stator and flux is important where it act as a feedback to the drive system. The value of phase voltage and phase current are obtained by switching pattern and measure by sensor respectively. The output of the estimator is the actual torque and actual flux that will be compared to the references torque and references flux of drive system. The benefit of this estimator is the limited parameter that is only phase voltages and currents required.

The voltage component which can be obtain by the switching pattern is express by the following equation [3.10] and [3.11] in the previous part. The current component is obtained by applying the Clarke's transformation using equation express in [3.15] and [3.16].

$$i_{sd} = i_a \quad (3.15)$$

$$i_{sq} = (i_a + 2i_b) / \sqrt{3} \quad (3.16)$$

The stator flux vector can be express in the stationary reference frame is given by [3.17].

$$\varphi_s = \int (v_s - i_s R_s) dt \quad (3.17)$$

Under steady state condition the equation may reduce to [3.18]

$$\varphi_s = \int (v_s - i_s R_s) dt / j\omega_e \quad (3.18)$$

The stator flux can be separated in phase component that is d-axis and q-axis given in [3.19] and [3.20].

$$\varphi_{sd} = \int (v_{sd} - i_{sd} R_s) dt \quad (3.19)$$

$$\varphi_{sq} = \int (v_{sq} - i_{sq} R_s) dt \quad (3.20)$$

The actual torque and actual flux equation is given by refer to the following equation as mention in [3.21] and [3.22].

$$T_e = \frac{3}{2} \mathcal{P} (\varphi_{sd} i_{sd} - \varphi_{sq} i_{sq}) \quad (3.21)$$

$$\varphi = \sqrt{(\varphi_{sd})^2 - (\varphi_{sq})^2} \quad (3.22)$$

3.2.3 Performing switching frequency calculation algorithm

This section will explain the construction of the switching frequency algorithm which uses to calculate the frequency of conventional inverter and CHMI. The result then will be compared in order to indicate clearly the advantages of proposed multilevel compared to the conventional.

Basically frequency is defined as repeating event per unit time. The SI unit use for the frequency is hertz (Hz). The switching frequency calculation is defined by summation of all switching of status, i.e. S_{a1} , S_{a2} , S_{b1} , S_{b2} , S_{c1} and S_{c2} divide by the sampling period of simulation. The equation is as mention in [3.23]

$$\text{Switching frequency (Hz)} = \frac{S_{a1} + S_{a2} + S_{b1} + S_{b2} + S_{c1} + S_{c2}}{\text{sampling period}, s} \quad (3.23)$$

However the sampling of the switching frequency will be taken during the steady state operation mode of the induction machine. The specific setting of speed will be set at the induction machine. After the motor reach the specific speed setting the algorithm will start to calculate. The sampling time will be different for each speed since high speed required more time before it can regulate.

The sampling time is kept constant at $1\mu s$ to ensure the ideal condition of the DTC system. By vary the torque hysteresis band and flux hysteresis band the sampling frequency will be recorded.

3.2.4 Simulation block model of DTC of induction machine utilizing CHMI

This part review the topology of DTC drive to illustrate the flow of decouples control structure. Figure 3.10 show the simulation block composes of many subsystems that important to perform the DTC. First and foremost, the look-up table which determine the selection of suitable voltage vectors or switching states $[S_{a1}, S_{a2}]$, $[S_{b1}, S_{b2}]$ and $[S_{c1}, S_{c2}]$ as tabulate in Table 3.2. This switching selection is to trigger the CHMI to perform the controlling of the induction machine. Besides that, the feedback part consists of the stator flux and electromagnetic torque which will produce actual flux and torque respectively. The switching algorithm part is important to determine the switching frequency of the drive system which helps to do the analysis of the inverter.

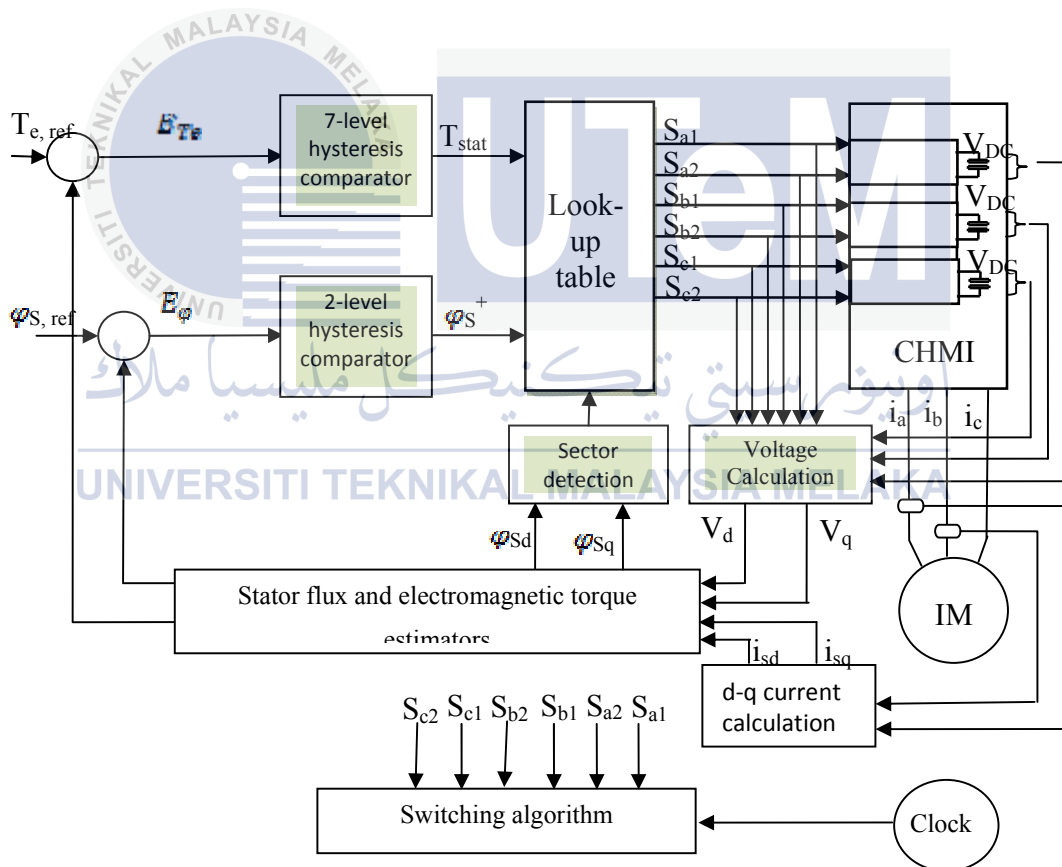


Figure 3.10: A de-couple control structure of DTC of induction machine using CHMI

3.2.5 Verification of the effectiveness of the simulation

This part review comparison of 3-level CHMI voltage space vector with the conventional 2-level voltage inverter. As shown in figure 3.11 (b), the higher number of multilevel inverter voltage, the more voltage vector are generated.

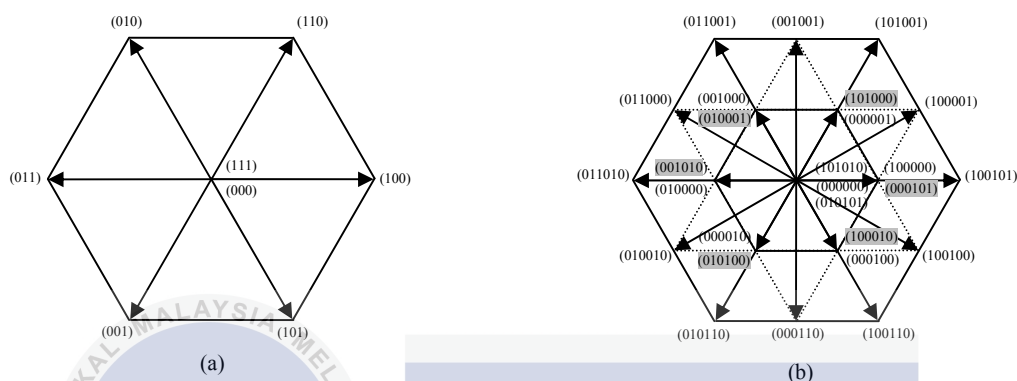


Figure 3.11: Voltage vectors available in (a) Conventional inverter and (b) CHMI

The correct strategy for selection of voltage vector is important to ensure brilliant controlling performance of induction machine. Based on the figure (a), it can be noted in conventional design only produced 6 effective voltage vectors. On the other hand, 3-level CHMI show three times generation of effective voltage vector that is 18 non-zero voltage vectors.

By increasing the selection choices for switching state, it actually decreases the switching frequency [1]. Decreasing in switching frequency will reduce the possibility of overshoot to happen hence reduce the percentages of total harmonic distortion (THD). This can be achieved when the switching frequency show great reduces in 3-level CHMI compared to the VSI.

3.3 Summary of methodology by flowchart

Figure 3.12 shows the summarized procedure of modeling the simulation and development of look-up table by flow chart in this chapter.

Flow chart of proposed research activities

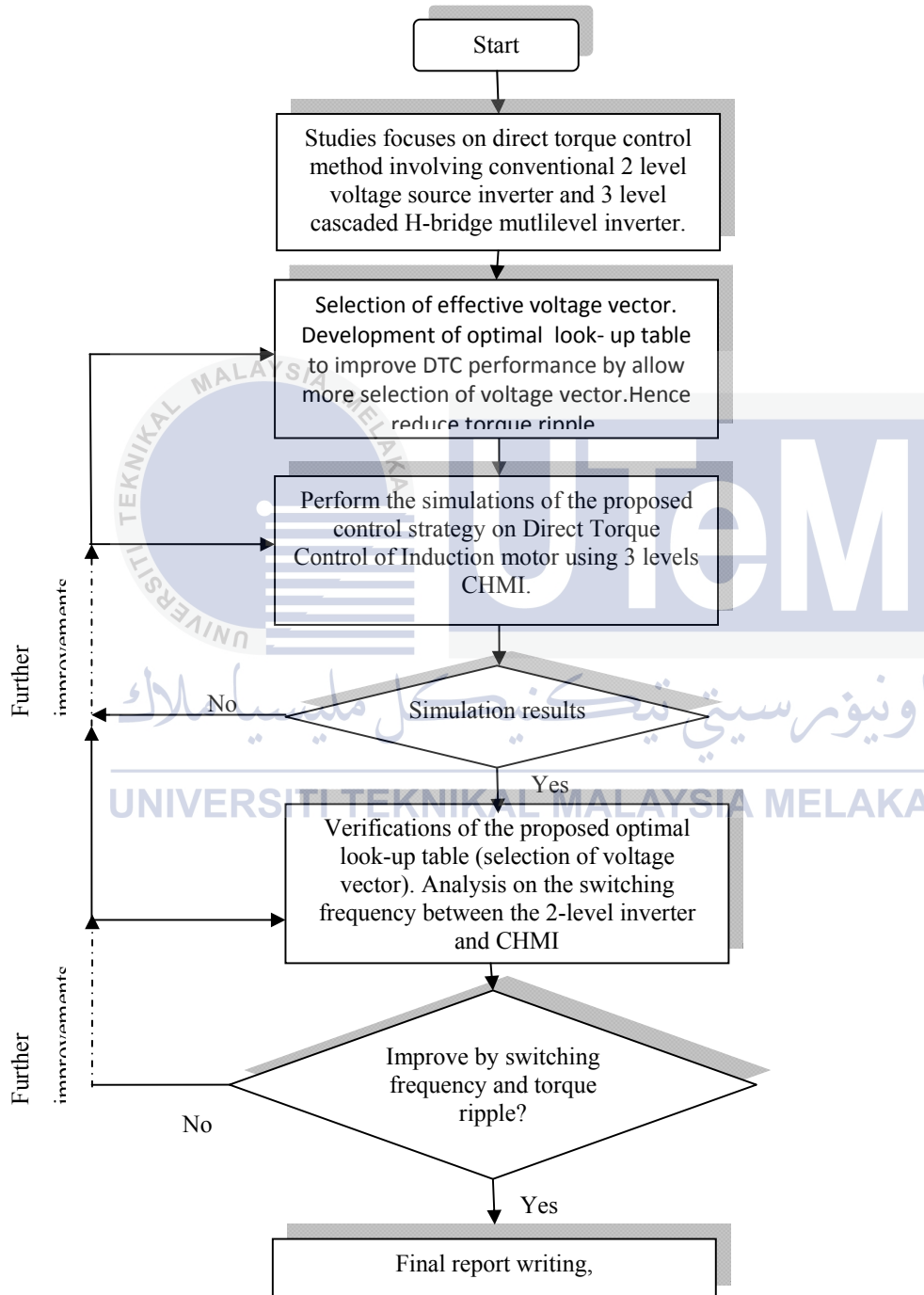


Figure 3.12: Summarization on procedure to construct optimum look-up table for CHMI

CHAPTER 4

RESULT

4.1 Introduction

This section will show the result of the previous work done in chapter 3. The final result will be based on direct torque control by comparing between the conventional inverter and cascaded H-bridge multilevel inverter (CHMI). The analysis of switching frequency and discussion of the result also will be cover in this chapter.

4.2 Simulation constructed using MATLAB

This simulation of DTC drive was carried out using Matlab/Simulink simulation package. Simulation show in Figure 4.1 was constructed based on the model shown in Figure 3.9. The construction of the simulation includes the insertion of formulated coding in block editor and mathematical equation that create a induction machine and related subsystem. Figure 4.2 shows a full design of DTC system which can perform both conventional and proposed condition by change the number of relay and it function block parameter. To apply the conventional inverter condition, the switching selection is based on long amplitude and short amplitude voltage space vector. In addition, to apply CHMI, the medium amplitude voltage space vector also includes.

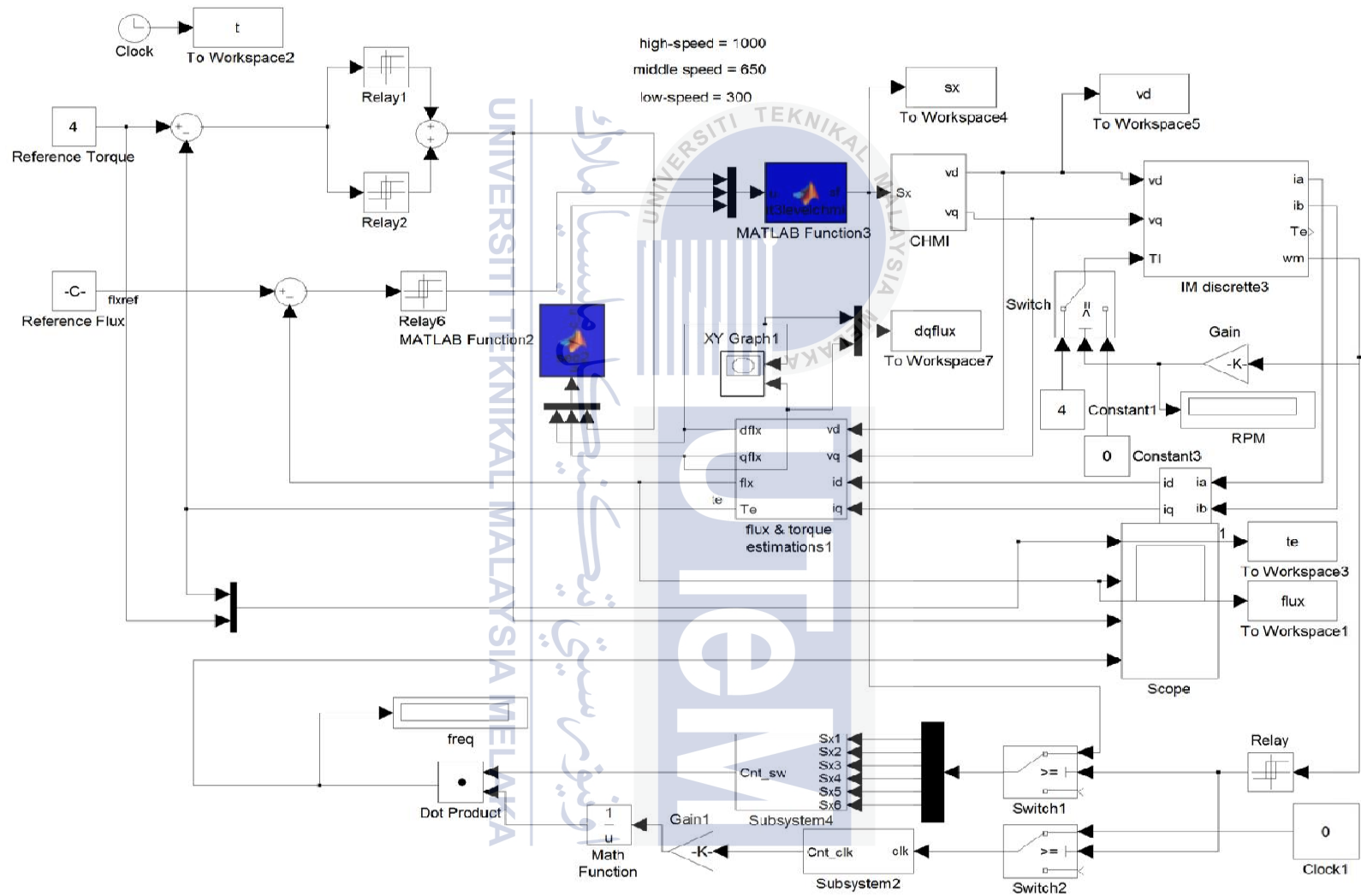


Figure 4.1: Simulation result on Matlab of a de-couple control structure of DTC utilizing CHMI on induction machine

4.3 Simulation results

The comparison between DTC utilizing conventional inverter and CHMI can be verified through the result. The simulation result was obtained to confirm the principle of the DTC strategy on conventional inverter and CHMI on induction machine. From the comparison, both systems were tested with same motor and control parameter as tabulated at Table 4.1.

Table 4.1: Motor and control parameter

Induction machine	
Rated power, P	1.1 kW
Rated voltage, V_s	380 V
Rated current, $i_{s,rated}$	2.7 A
Rated speed, ω_m	2800 rpm
Stator resistance, R_s	6.1 Ω
Rotor resistance, R_r	4.51 Ω
Stator self inductance, L_s	306.5 mH
Rotor self inductance, L_r	306.5 mH
Mutual inductance, L_m	291.9 mH
Combined inertia, J	0.0565 kg-m ²
Combined viscous friction, B	0.0245 N.m.s
Number of pole pairs, P	2
Control parameter	
Sampling period	1 μ s
Direct current voltage, V_{dc}	120 V
Torque rated	4 Nm
Flux rated	0.8452 Wb

Figure 4.2 shows the comparison of torque control performance obtained for multistep change of $T_{e, \text{ref}}$ from 1 Nm at $t = 0$ s to $t = 0.25$ s then to 2 Nm before to change to 4 Nm at $t = 0.5$ s. From the figure provided it can be seen clearly that selection of voltage vector has varies according to the torque demands. In this case the torque hysteresis band and flux hysteresis band are set at 0.5 and 0.01 respectively. It can be seen that Figure 4.2 (a) has thick torque response compare to Figure 4.2 (b). This is because the different selection of voltage vector in conventional inverter and CHMI. In conventional inverter, the selections of voltage only consist of long amplitude voltage vector at any speed. On the other hand, in CHMI, the selections are depending on different amplitude of effective voltage vector based on the speed of the induction machine that is low, medium or high speed. By applying CHMI, it prevent extreme torque change which will result reduce in torque ripple. In order to provide better picture, zoom image provided in Figure 4.3 prove that the rate of torque increase in conventional inverter is more than CHMI. By having selection of vector through the proposed strategy allows the hysteresis band to be reduced hence lead to the decrease in torque response.

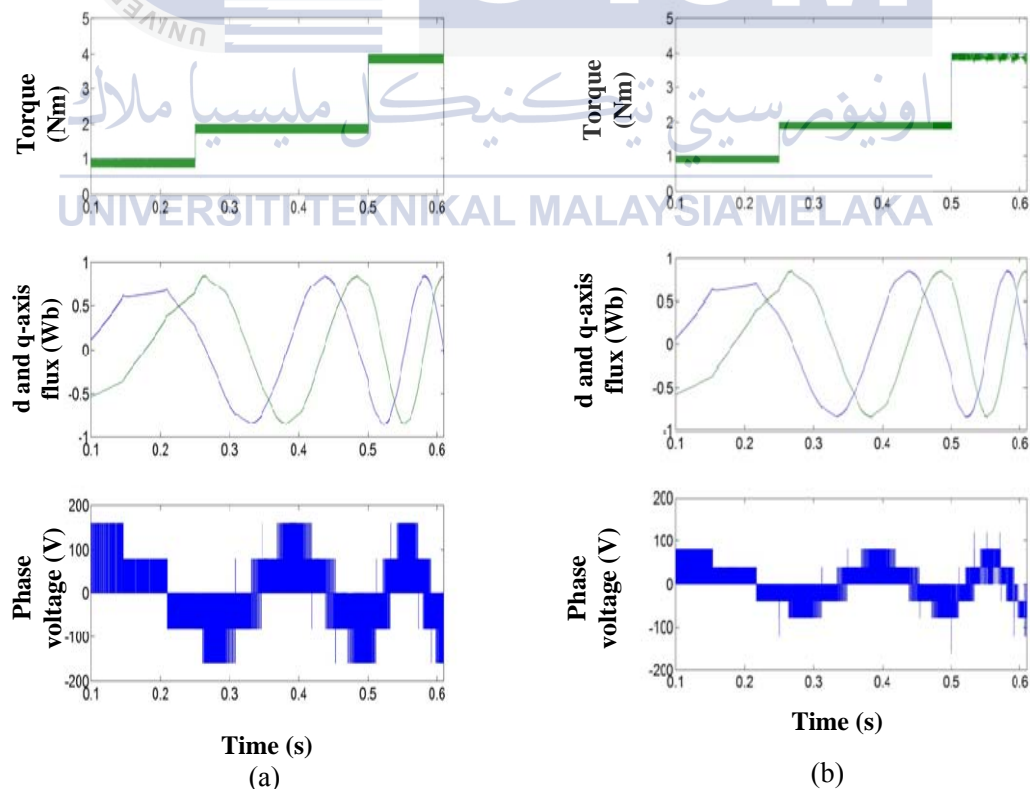


Figure 4.2: Performance comparison of torque control based on selection of vectors using (a) 2-level inverter (b) CHMI

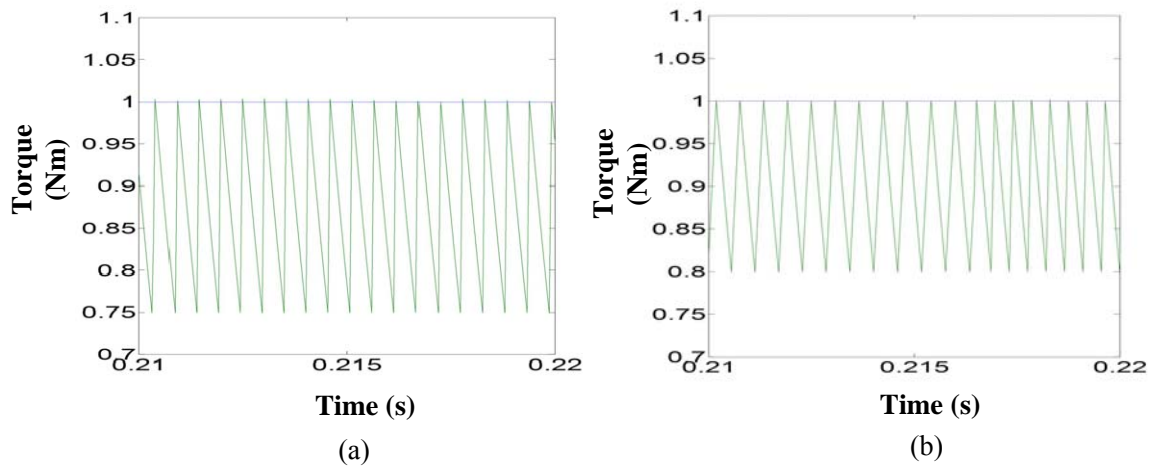


Figure 4.3: Magnified simulation result obtain (a) conventional inverter (b) CHMI

4.4 Data tabulation of switching frequency

In order to achieve high performance of DTC it is important to choose the most suitable torque and flux band. The analysis is to verify the improvement in term of switching frequency of DTC using conventional inverter and CHMI. This is done by varies the torque hysteresis band, flux hysteresis band and speed condition. Generally, current distortion and torque ripple can be reduce by choose the small flux hysteresis and small torque hysteresis respectively. However this condition may lead to high switching frequency since the band is reduce.

To collect the switching frequency data, the DTC is set to have constant torque reference and constant flux reference that is 4 Nm and 0.8452 Wb respectively. The speed is set at 3 different speeds, i.e. 300 rpm, 650 rpm and 1000 rpm; torque hysteresis bands, i.e. 5%, 10%, 15%, 20% and 25% of torque rated, and flux hysteresis bands, i.e. 0.2%, 0.4%, 0.6%, 0.8%, 1.0%, 1.2% and 1.4% of rated flux. The sampling period of the simulation were set at $0.3\mu\text{s}$, $0.5\mu\text{s}$ and $0.7\mu\text{s}$ for speed 300 rpm, 650 rpm and 1000 rpm respectively. The data collected from this simulation were presented in three dimensional graphs (3D).

The switching frequency calculation is defined by summation of all switching status, i.e. S_{a1} , S_{a2} , S_{b1} , S_{b2} , S_{c1} and S_{c2} divide by the sampling period of simulation. This part will show the data that collected by varying of flux and torque hysteresis band. The tabulation of data using conventional inverter and CHMI was carried out in three conditions; low, medium and high speed of motor. The condition of the conventional inverter based on the voltage selection; $V_{highzero}$ and the condition of the CHMI based on the voltage selection; $V_{lowzero}$, $V_{mediumlow}$ and $V_{lowhigh}$.

The variations of test condition are defined as follows:

Conventional (V_{HZ}) : During the operation, in order to increase torque it will choose the high active forward voltage vector but to decrease the torque, the zero amplitude voltage vector is selected.

CHMI (V_{LZ}) : During the low speed operation, in order to increase torque it will choose the low active forward voltage vector but to decrease the torque, the zero amplitude voltage vector is selected.

CHMI (V_{ML}) : During the medium speed operation, in order to increase torque it will choose the medium active forward voltage vector but to decrease the torque, the low amplitude voltage vector is selected.

CHMI (V_{LH}) : During the high speed operation, in order to increase torque it will choose the high active forward voltage vector but to decrease the torque, the low active voltage vector is selected.

Tables below provided the switching frequency that generated after the rated torque, rated flux and sampling time kept constant. The Table 1, Table 3 and Table 5 state the condition of using conventional inverter while Table 2, Table 4 and Table 6 state the condition using CHMI with speed of 300 rpm, 650 rpm and 1000 rpm respectively.

- a) Condition : Conventional (V_{HZ})
 Period : 0.3 second

Table 4.2: Switching frequency (Hz) at 300 rpm

Flux Hysteresis Band	Torque Hysteresis Band					
		5%	10%	15%	20%	25%
0.2 %	45090 Hz	29810 Hz	22600 Hz	19970 Hz	17130 Hz	
0.4 %	34100 Hz	22480 Hz	16340 Hz	14690 Hz	13090 Hz	
0.6 %	31130 Hz	18600 Hz	14630 Hz	12940 Hz	10080 Hz	
0.8 %	30000 Hz	16780 Hz	12820 Hz	10340 Hz	9720 Hz	
1.0 %	29320 Hz	16130 Hz	11870 Hz	9630 Hz	8100 Hz	
1.2 %	28630 Hz	15530 Hz	11270 Hz	9240 Hz	8110 Hz	
1.4 %	28570 Hz	15340 Hz	10900 Hz	8700 Hz	7510 Hz	

- b) Condition : CHMI (V_{LZ})
 Period : 0.3 second

Table 4.3: Switching frequency (Hz) at 300 rpm

Flux Hysteresis Band	Torque Hysteresis Band					
		5%	10%	15%	20%	25%
0.2 %	27690 Hz	26680 Hz	25720 Hz	24970 Hz	24150 Hz	
0.4 %	15050 Hz	14200 Hz	13650 Hz	13050 Hz	12730 Hz	
0.6 %	10970 Hz	10010 Hz	9590 Hz	9170 Hz	8830 Hz	
0.8 %	8680 Hz	7910 Hz	7440 Hz	7150 Hz	6760 Hz	
1.0 %	7420 Hz	6530 Hz	6220 Hz	5980 Hz	5810 Hz	
1.2 %	6560 Hz	5700 Hz	5350 Hz	5170 Hz	4910 Hz	
1.4 %	5950 Hz	5070 Hz	4820 Hz	4520 Hz	4390 Hz	

- c) Condition : Conventional (V_{HZ})
 Period : 0.5 second

Table 4.4: Switching frequency (Hz) at 650 rpm

Flux Hysteresis Band	Torque Hysteresis Band				
		5%	10%	15%	20%
0.2 %	44880 Hz	34470 Hz	28000 Hz	26200 Hz	25790 Hz
0.4 %	34060 Hz	22590 Hz	18440 Hz	17110 Hz	14810 Hz
0.6 %	30810 Hz	20690 Hz	14980 Hz	13470 Hz	12080 Hz
0.8 %	28570 Hz	17360 Hz	13500 Hz	11580 Hz	10650 Hz
1.0 %	27630 Hz	16160 Hz	12260 Hz	10270 Hz	8850 Hz
1.2 %	26660 Hz	15330 Hz	11540 Hz	9720 Hz	8260 Hz
1.4 %	26300 Hz	15020 Hz	11150 Hz	9130 Hz	8350 Hz

- d) Condition : CHMI (V_{ML})
 Period : 0.5 second

Table 4.5: Switching frequency (Hz) at 650 rpm

Flux Hysteresis Band	Torque Hysteresis Band				
		5%	10%	15%	20%
0.2 %	26300 Hz	15020 Hz	11150 Hz	9130 Hz	8350 Hz
0.4 %	23790 Hz	18590 Hz	17120 Hz	16230 Hz	15640 Hz
0.6 %	20670 Hz	14740 Hz	12820 Hz	11910 Hz	11090 Hz
0.8 %	17730 Hz	11360 Hz	10440 Hz	9330 Hz	9020 Hz
1.0 %	16130 Hz	11350 Hz	8760 Hz	8730 Hz	7520 Hz
1.2 %	15220 Hz	10190 Hz	7670 Hz	6930 Hz	6770 Hz
1.4 %	14770 Hz	10110 Hz	8370 Hz	5920 Hz	5810 Hz

- e) Condition : Conventional (V_{HZ})
 Period : 0.7 second (High speed)

Table 4.6: Switching frequency (Hz) at 1000 rpm

Flux Hysteresis Band	Torque Hysteresis Band				
	5%	10%	15%	20%	25%
0.2 %	38550 Hz	33010 Hz	31450 Hz	29930 Hz	29190 Hz
0.4 %	24650 Hz	19440 Hz	17790 Hz	16850 Hz	16220 Hz
0.6 %	20200 Hz	14970 Hz	13340 Hz	12420 Hz	11890 Hz
0.8 %	17920 Hz	12840 Hz	11310 Hz	10450 Hz	9610 Hz
1.0 %	16580 Hz	11380 Hz	9770 Hz	8900 Hz	8290 Hz
1.2 %	15790 Hz	10530 Hz	8850 Hz	7810 Hz	7270 Hz
1.4 %	14770 Hz	9730 Hz	8080 Hz	7240 Hz	6690 Hz

- f) Condition : CHMI (V_{LH})
 Period : 0.7 second (High speed)

Table 4.7: Switching frequency (Hz) at 1000 rpm

Flux Hysteresis Band	Torque Hysteresis Band				
	5%	10%	15%	20%	25%
0.2 %	34640 Hz	32460 Hz	31300 Hz	31120 Hz	30790 Hz
0.4 %	18930 Hz	16930 Hz	16850 Hz	16360 Hz	16100 Hz
0.6 %	14170 Hz	12730 Hz	12420 Hz	11640 Hz	11340 Hz
0.8 %	11590 Hz	9790 Hz	9440 Hz	9140 Hz	9250 Hz
1.0 %	10420 Hz	8580 Hz	7950 Hz	7590 Hz	7570 Hz
1.2 %	9590 Hz	7370 Hz	7260 Hz	6411 Hz	6330 Hz
1.4 %	8660 Hz	7030 Hz	6120 Hz	5764 Hz	5370 Hz

4.5 Three dimensional graph representation

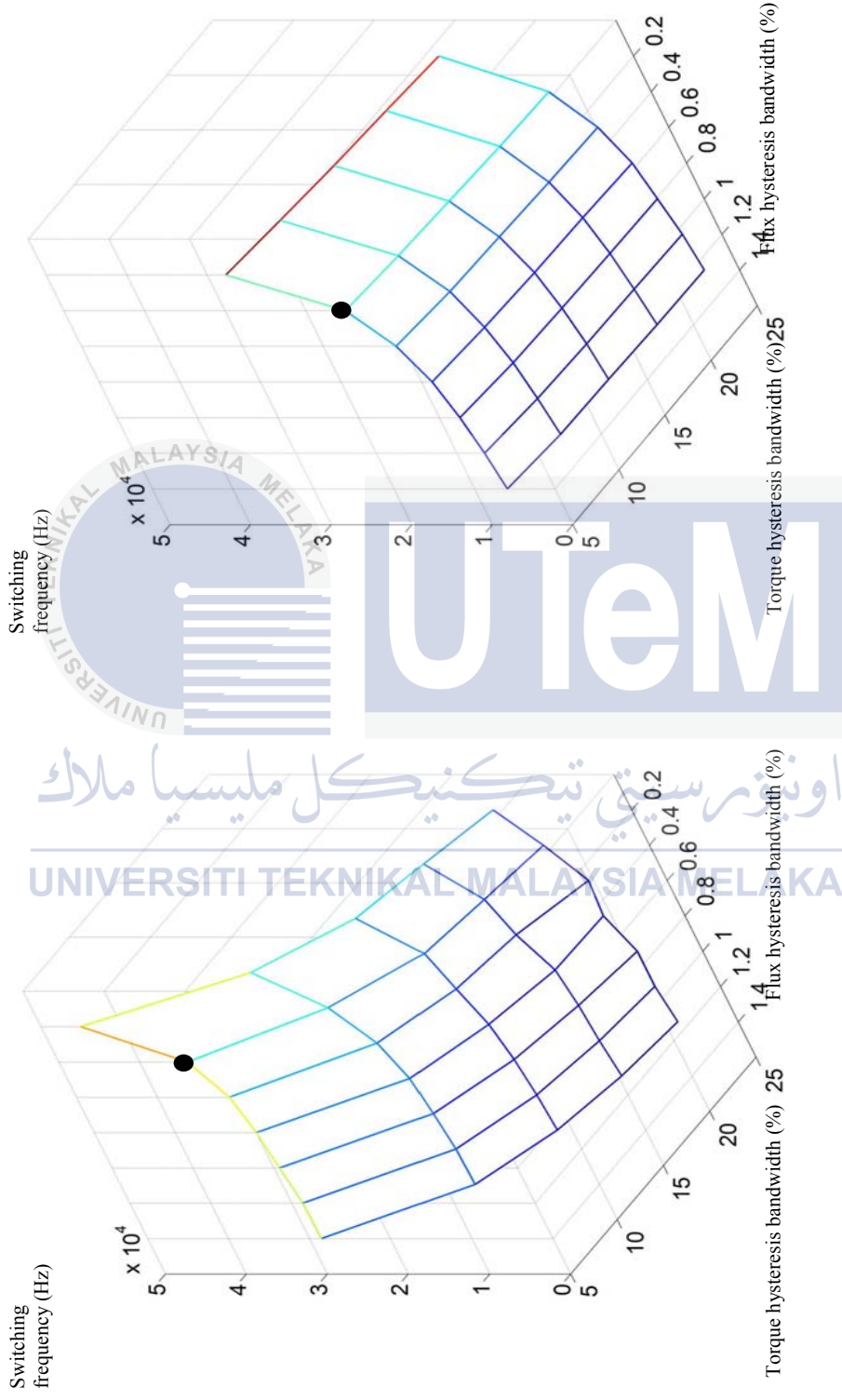
This part represents the data collected in (3D) graph in order to compare between the conventional inverter and CHMI performance. Based on the result plotted in Figure 4.4, at the point 5 % of torque hysteresis band and 0.2 % of the flux hysteresis band, the conventional inverter show the highest switching frequency. By using the same condition but applying

using CHMI the switching frequency has reduces almost 61 %. At the point 25 % of torque hysteresis band and 1.4% of the flux hysteresis band, the CHMI show the lowest switching frequency that is 4390 Hz that is reduce by 58 % compare to the conventional inverter. This show that by having smaller percentage of torque band and flux band may lead to the increasing in switching frequency.

By analysis the result plotted in Figure 4.5, at the point 5 % of torque hysteresis band and 0.2 % of the flux hysteresis band, the conventional inverter show the highest switching frequency that is 44880 Hz. By using the same condition but applying using CHMI the switching frequency has reduces almost 59 %. At the point 25 % of torque hysteresis band and 1.4% of the flux hysteresis band, the CHMI show the lowest switching frequency that is 5810 Hz that is reduce by 69 % compare to the switching frequency of conventional inverter.

Last but not least, based on Figure 4.6, where the operation speed is at highest the switching frequency decreasing was insignificant. At the point 5 % of torque hysteresis band and 0.2 % of the flux hysteresis band, the conventional inverter record the reading of 38550 Hz while the CHMI record 34640 Hz. The percentage of switching frequency reduce is about 10% only.

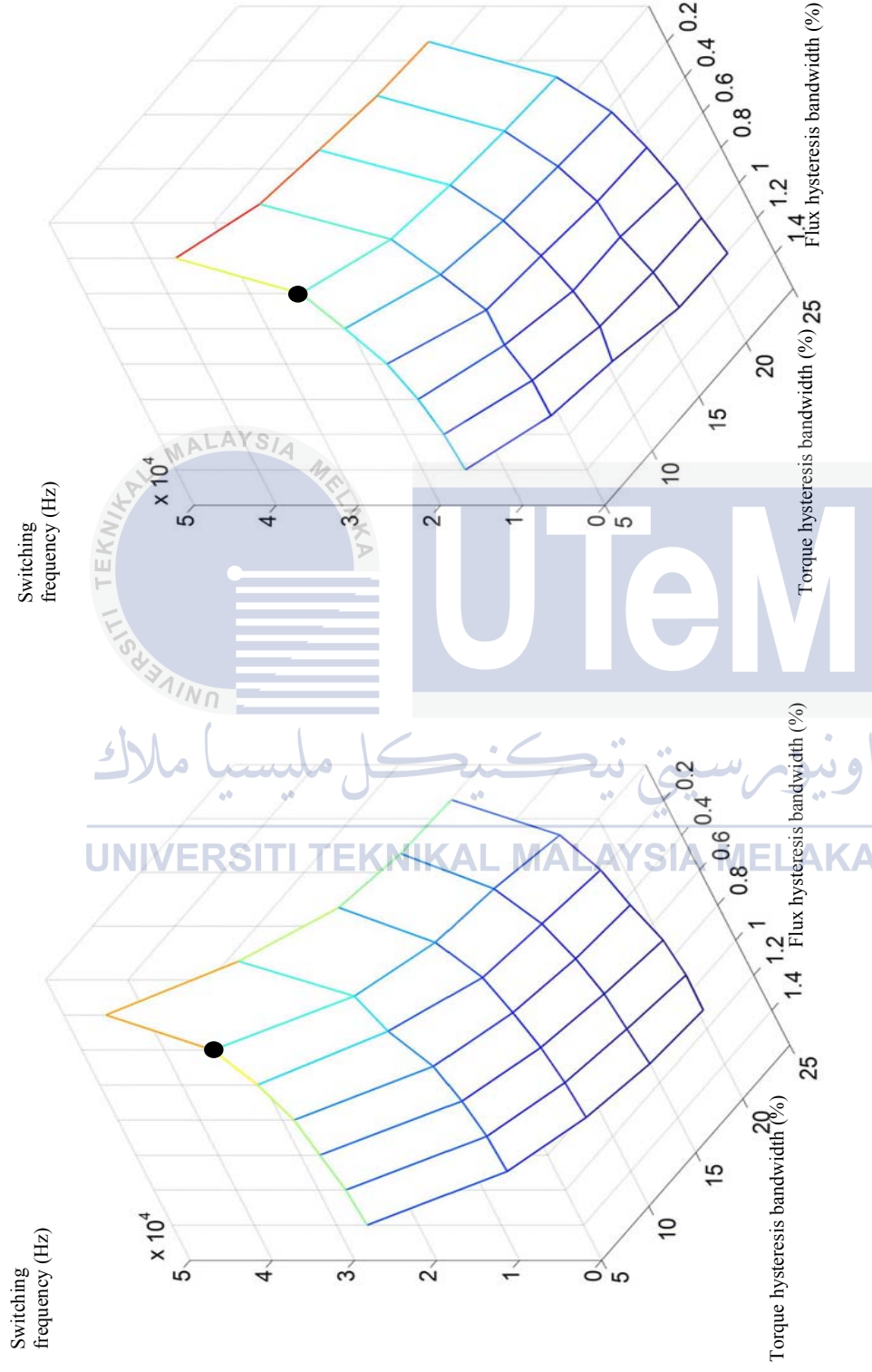
By observing the three speed condition, lower speed operation show the significant change of switching frequency compared to the medium and high speed operation. This is because the selection of appropriate voltage amplitude in low speed that is V_{LZ} compared to the V_{HZ} . On the other hand the high speed operation show insignificant change because the selection of V_{LH} . Although the decrement in CHMI was insignificant as the torque hysteresis band increase but it was significant during the flux hysteresis band increase.



(a)

(b)

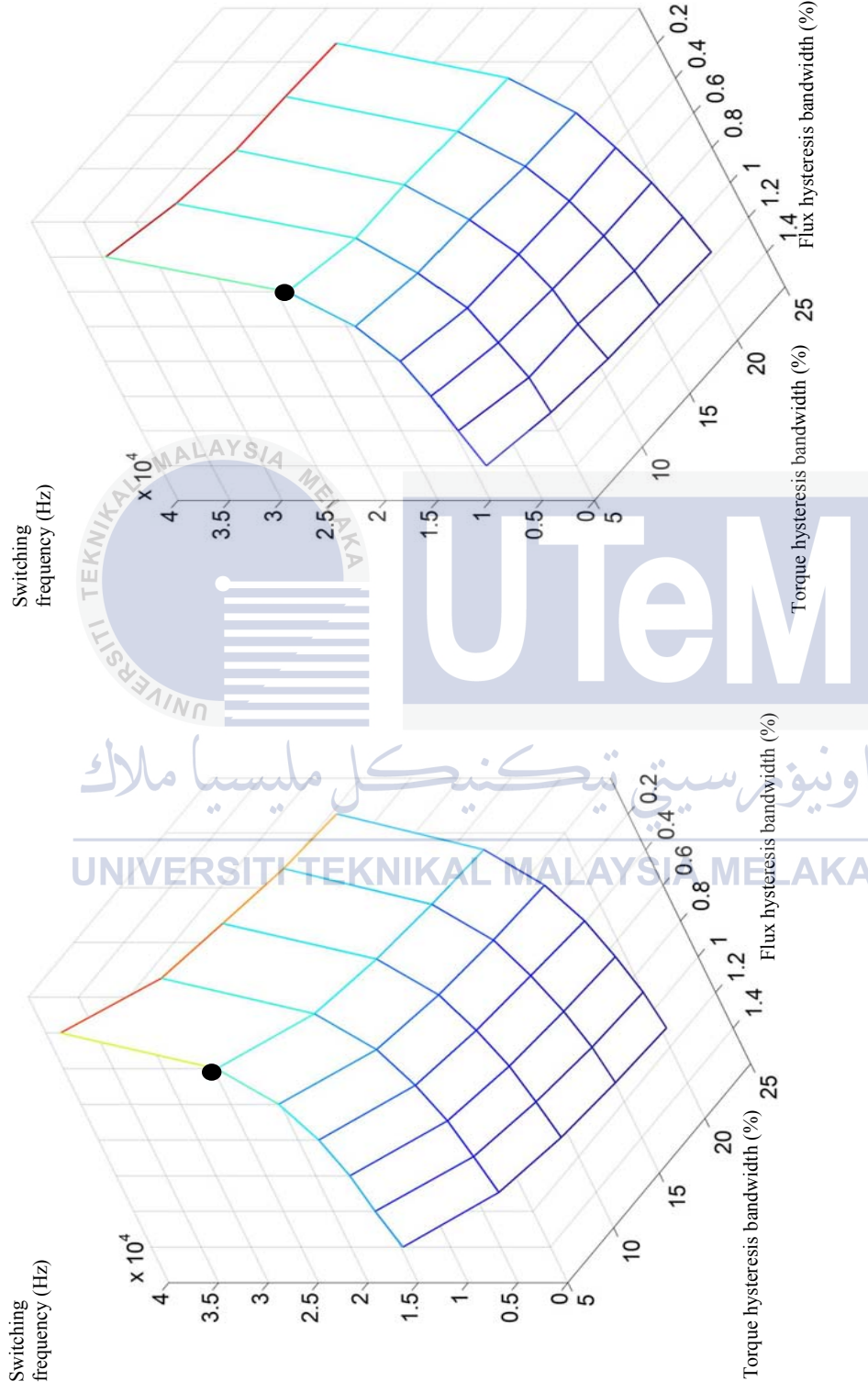
Figure 4.4: Switching frequency variation at 300 rpm (a) Conventional (V_{HL}) (b) CHMI (V_{HL})



(a)

(b)

Figure 4.5: Switching frequency variation at 650 rpm (a) Conventional (V_{HZ}) (b) CHMI (V_{HL})



(a)

Figure 4.6: Switching frequency variation at 1000 rpm (a) Conventional (V_{HZ}) (b) CHMI (V_{HL})

4.6 Waveform result

This part will show the waveform of the simulation in term of torque response and phase voltage. As mark by dot in the Figure 4.4-Figure 4.6, the hysteresis band for torque and flux is set at 5% and 0.4% respectively from the rated.

Based on Figure 4.7 (a) it can be seen that the conventional inverter has higher rate of change voltage compared to the Figure 4.7 (c) using CHMI. From the observation at zoom image result at Figure 4.7 (b), it can be seen that the slope of torque for conventional inverter was closely compared to the Figure 4.7 (d). This indicates the faster switching frequency and also the rapid change in slope of torque to increase and decrease. In this situation, the IGBT or MOSFET will on / off very speedily and chance in possibility to damage is high. Besides that, by using the conventional inverter, it produces the highest switching frequency and dv/dt will be stress. When the switching frequency is high, the possibility the switching losses will be happen and affect to the performance of inverter and the machine. It is also obvious can be seen that using CHMI the change in slope increase and decrease a bit slow, since the appropriate selection of voltage vector has increase. Besides that, it can be highlighted that the dv/dt has reduce.

Based on Figure 4.8 (a) and Figure 4.9 (a), it can be seen that the conventional inverter has higher rate of change voltage compared to the Figure 4.8 (c) and Figure 4.9 (c). From the observation at zoom image result at Figure 4.8 (b), it can be seen that the slope of torque for conventional inverter was closely compared to the Figure 4.8 (d). However, in Figure 4.9 (b) and Figure 4.9 (d), the slope of torque using conventional inverter almost the same as using CHMI.

By observing overall speed the improvement of torque ripple was higher during low speed since the improvement of the switching frequency by 44 % compared when using the conventional inverter. The significant of improvement tend to decrease as the speed increase.

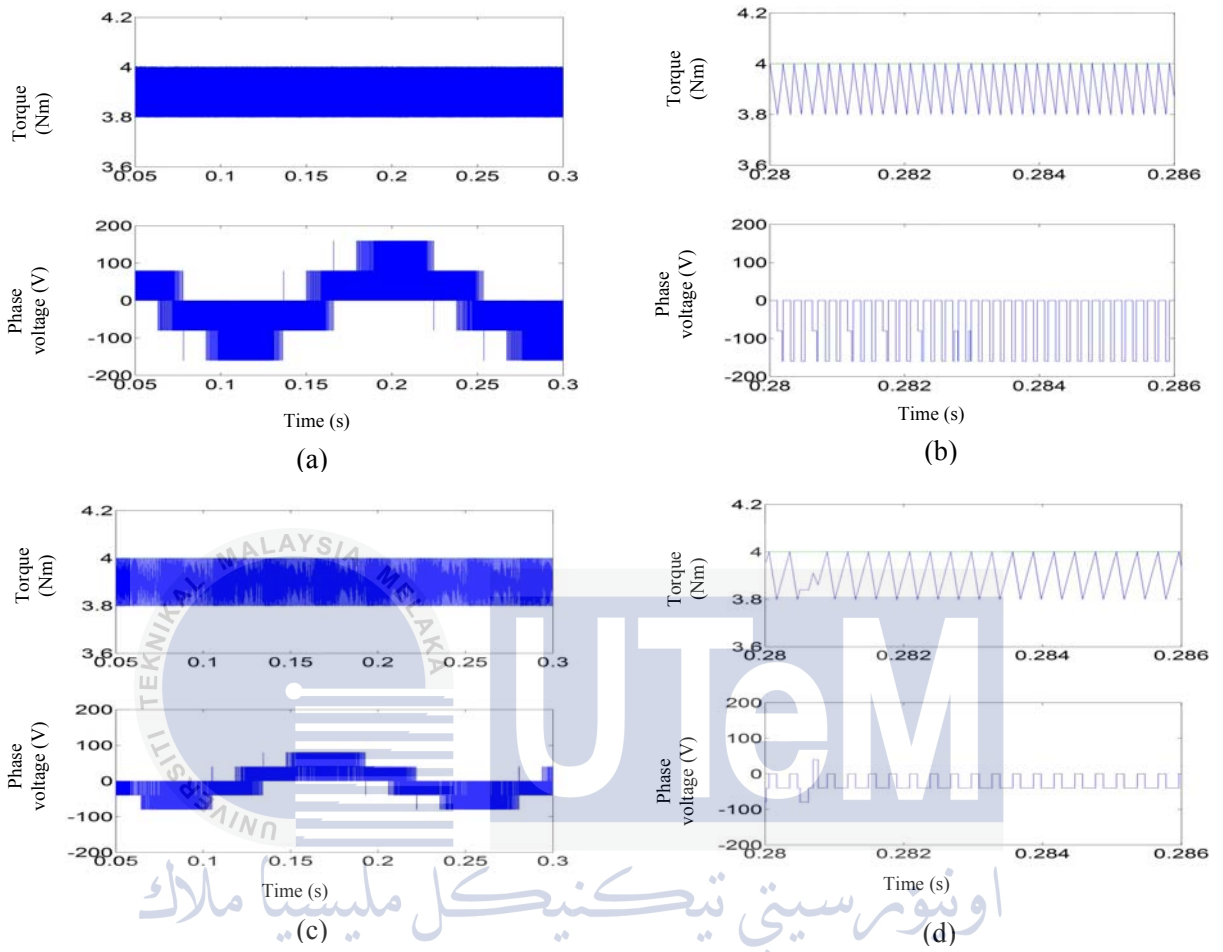
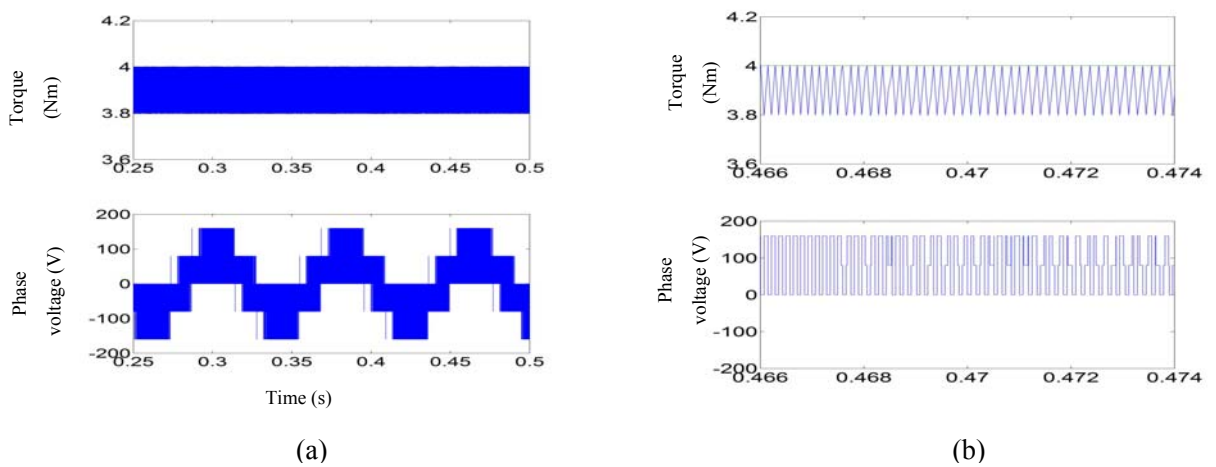
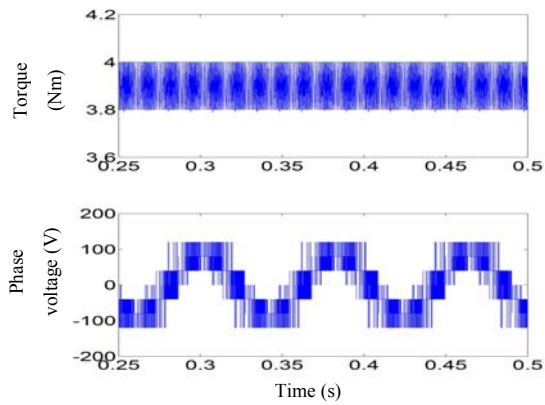
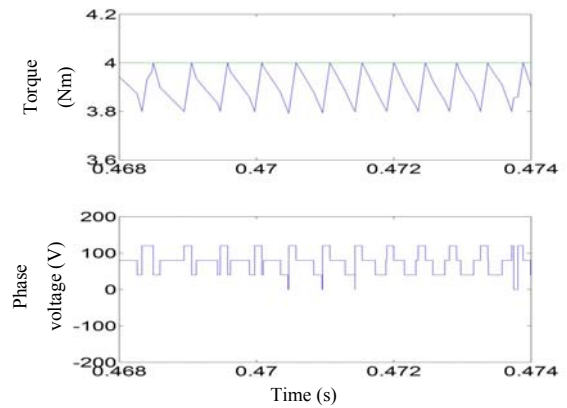


Figure 4.7: Comparison the switching frequency at low speed operation. (a) Conventional inverter (b) zoom image of conventional inverter (c) CHMI (d) zoom image of CHMI



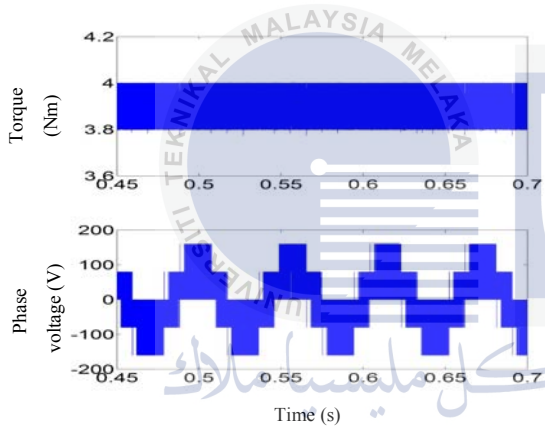


(c)

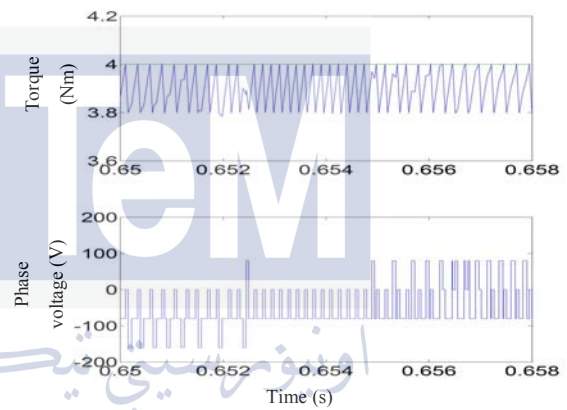


(d)

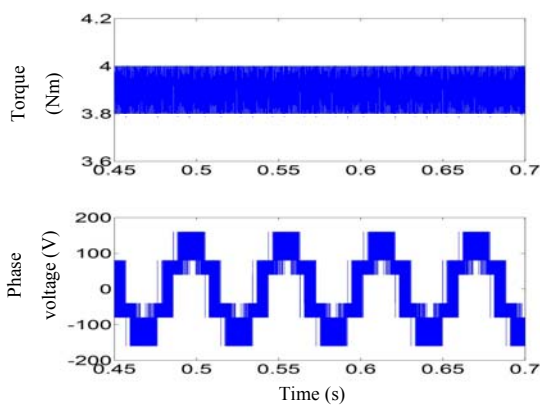
Figure 4.8: Comparison the switching frequency at medium speed operation. (a) Conventional inverter (b) zoom image of conventional inverter (c) CHMI (d) zoom image of CHMI



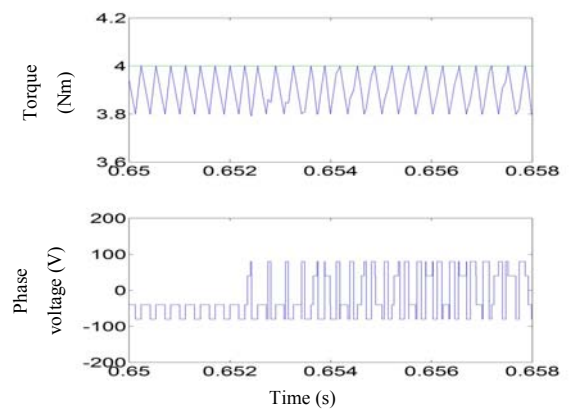
(a)



(b)



(c)



(d)

Figure 4.9: Comparison the switching frequency at high speed operation. (a) Conventional inverter (b) zoom image of conventional inverter (c) CHMI (d) zoom image of CHMI

CONCLUSION & RECOMMENDATION

5.1 Conclusion

In a nut shell, this project achieved the objective highlighted at first chapter. The development of optimal look-up table have been achieved since it produce 19 effective voltage vector which give better selection in order to improve DTC. By having appropriate selection of voltage vector, the switching frequency will be reduce especially during changes of speed occur on induction machine. In addition, by constructing the DTC utilizing CHMI, the result shows some improvement in reducing the torque ripple and switching frequency. The last part of the analysis also highlighted the zoom image of torque ripple waveform between conventional inverter and CHMI which show decreasing in dv/dt stress. Since the improvement has been achieved, it is encourage that DTC method to use multilevel inverter compared to the conventional inverter. This is because the advantages using inverter with more level is that they provide and produce better approximation of sine wave (lower harmonic contain).

5.2 Recommendation

In this project, although multilevel has provide be several advantages highlighted in previous section, it also may disadvantages such as developing more levels required higher manufacturing cost. In order to reduce the cost, studies on the new topology inverter which

constructed with less switching device must be done. Besides that, during the analysis of switching frequency, it is being done manually follow the condition set based on the low, medium and high speed operation. In order to improve this, the torque performance should be automatically changed by applying the multistep change.



REFERENCES

1. Ahmadi, M. Z. R. Z. J., A. ; Binti Jaffar, K. ; Othman, M.N. ; Nagarajan, R.N.P. ; Jopri, M.H. . (2013). Minimization of torque ripple utilizing by 3-L CHMI in DTC. *Power Engineering and Optimization Conference (PEOCO), 2013 IEEE 7th International*, 636- 640.
2. Takahashi, I., & Noguchi, T. (1986). A New Quick-Response and High-Efficiency Control Strategy of an Induction Motor. *Industry Applications, IEEE Transactions on, IA-22(5)*, 820-827. doi: 10.1109/TIA.1986.4504799
3. Hoang, L.-H. (1999, 1999). *Comparison of field-oriented control and direct torque control for induction motor drives*. Paper presented at the Industry Applications Conference, 1999. Thirty-Fourth IAS Annual Meeting. Conference Record of the 1999 IEEE.
4. Ceglia, G., Guzman, V., Sanchez, C., Ibanez, F., Walter, J., & Gimenez, M. I. (2006). A New Simplified Multilevel Inverter Topology for DC–AC Conversion. *Power Electronics, IEEE Transactions on, 21(5)*, 1311-1319. doi: 10.1109/TPEL.2006.880303
5. Haitham Abu-Rud, Atif Iqbal & J.Guzinski, (2012). High performance control of AC Drives. 1st edition, United Kingdom: A John Wiley & Sons Ltd.
6. Nabae, A., Takahashi, I., & Akagi, H. (1981). A New Neutral-Point-Clamped PWM Inverter. *Industry Applications, IEEE Transactions on, IA-17(5)*, 518-523. doi: 10.1109/TIA.1981.4503992
7. Kang, D. W., Ma, C. S., Kim, T. J., & Hyun, D. S. (2004). Simple control strategy for balancing the DC-link voltage of neutral-point-clamped inverter at low modulation index. *Electric Power Applications, IEE Proceedings -, 151(5)*, 569-575. doi: 10.1049/ip-epa:20040543
8. Ganatra, D. H., & Pandya, S. N. (2012, 1-2 March 2012). *Torque ripple minimization in Direct Torque Control based induction motor drive using multilevel inverter*. Paper presented at the Electrical, Electronics and Computer Science (SCEECS), 2012 IEEE Students' Conference on.
9. Priyan, S. S., & Ramani, K. (2013, 6-8 Feb. 2013). *Implementation of closed loop system for flying capacitor multilevel inverter with stand-alone Photovoltaic input*. Paper presented at the Power, Energy and Control (ICPEC), 2013 International Conference on.

10. Khoucha, F., Lagoun, S. M., Marouani, K., Kheloui, A., & El Hachemi Benbouzid, M. (2010). Hybrid Cascaded H-Bridge Multilevel-Inverter Induction-Motor-Drive Direct Torque Control for Automotive Applications. *Industrial Electronics, IEEE Transactions on*, 57(3), 892-899. doi: 10.1109/TIE.2009.2037105
11. Sung-Geun, S., Feel Soon, K., & Sung-Jun, P. (2009). Cascaded Multilevel Inverter Employing Three-Phase Transformers and Single DC Input. *Industrial Electronics, IEEE Transactions on*, 56(6), 2005-2014. doi: 10.1109/TIE.2009.2013846
12. Gupta, K. K., Kumar, L., & Jain, S. (2012, 16-19 Dec. 2012). *A new seven-level hybrid inverter*. Paper presented at the Power Electronics, Drives and Energy Systems (PEDES), 2012 IEEE International Conference on.
13. Azli, N. A., & Choong, Y. C. (2006, 28-29 Nov. 2006). *Analysis on the Performance of a Three-phase Cascaded H-Bridge Multilevel Inverter*. Paper presented at the Power and Energy Conference, 2006. PECon '06. IEEE International.
14. Bin Raja Yunus, R. N. A., Jidin, A., Alias, N. F., Herlino, A. L., & Manap, M. (2013, 26-29 Oct. 2013). *Performance analysis of direct torque control of induction machines*. Paper presented at the Electrical Machines and Systems (ICEMS), 2013 International Conference on.
15. Mortezaei, A. A., N.A. ; Idris, N.R.N. ; Mahmoodi, S. ; Nordin, N.M. . Direct torque control of induction machines utilizing 3-level cascaded H-Bridge Multilevel Inverter and fuzzy logic. *Applied Power Electronics Colloquium (IAPEC), 2011 IEEE*, 116-121.
16. Patil, U. V., Suryawanshi, H. M., & Renge, M. M. (2012, 30-31 March 2012). *Performance comparison of DTC and FOC induction motor drive in five level diode clamped inverter*. Paper presented at the Advances in Engineering, Science and Management (ICAESM), 2012 International Conference on.
17. Jidin, A., Idris, N. R. N., & Yatim, A. H. M. (2008b, 1-3 Dec. 2008). *A quick dynamic torque control for direct torque control hysteresis-based induction machines*. Paper presented at the Power and Energy Conference, 2008. PECon 2008. IEEE 2nd International.
18. Jidin, A., Idris, N., Yatim, A. H. M., & Elbuluk, M. (2008, 5-9 Oct. 2008). *A Novel Overmodulation and Field Weakening Strategy for Direct Torque Control of Induction Machines*. Paper presented at the Industry Applications Society Annual Meeting, 2008. IAS '08. IEEE.
19. Jidin, A., Idris, N. R. N., Yatim, A. H. M., & Elbuluk, M. E. (2009, 20-24 Sept. 2009). *A wide-speed high torque capability utilizing overmodulation strategy for direct torque control of induction machines*. Paper presented at the Energy Conversion Congress and Exposition, 2009. ECCE 2009. IEEE.

20. Jidin, A., Idris, N. R. N., & Yatim, A. H. M. (2008c, 1-3 Dec. 2008). *A simple overmodulation strategy in DTC-hysteresis based induction machine drives*. Paper presented at the Power and Energy Conference, 2008. PECon 2008. IEEE 2nd International.
21. Jidin, A., Idris, N. R. N., & Yatim, A. H. M. (2008a, 14-17 Dec. 2008). *A fast dynamic torque control for direct torque control hysteresis-based induction machines*. Paper presented at the Power Engineering Conference, 2008. AUPEC '08. Australasian Universities.
22. Babaei, E., Haque, M. T., & Hosseini, S. H. (2005, 29-29 Sept. 2005). *A novel structure for multilevel converters*. Paper presented at the Electrical Machines and Systems, 2005. ICEMS 2005. Proceedings of the Eighth International Conference on.



APPENDIX A



Project Planning

List major activities involved in the proposed project. Indicate duration of each activity to the related month(s).

Project Activities	Weeks														
	1	2	3	4	5	6	7	8	9	10	11	12	13	14	15
FYP 1	Sept.	Sept.	Sept.	Oct.	Oct.	Oct.	Oct.	Nov.	Nov.	Nov.	Nov.	Dec.	Dec.	Dec.	Dec.
Selecting the title for the project															
Identify the objective and scope															
Doing log book, research, study and pre design							1★								
Construction of look-up table (open loop)											2★				
Progress report															
FYP 2	Feb.	Mac.	Mac.	Mac.	Apr.	Apr.	Apr.	Apr.	Apr.	May	May	May	May	June	June
Construction of CHMI multilevel inverter							3★								
Construction of complete DTC control (closed loop)								4★							
Verification of the finding, discussion and analysis															
Result															
Report															

Milestones

- ★ 1 Comprehensive of various control strategy investigation and problems identification for Direct Torque Control (DTC) for induction machine using cascaded H-bridge multilevel inverter
- ★ 2 Completion in development of optimal look-up table
- ★ 3 Completed the design of 3L- CHMI
- ★ 4 Performing switching algorithm analysis